REDUCTION IN THERMAL RESISTANCE OF RESIDENTIAL WALL ASSEMBLIES BASED ON SIZE AND DISTRIBUTION OF VOIDS IN TWO TYPES OF INSULATION

A Thesis
by
HELEN WHISTLER BURKETT

Submitted to the Graduate School
at Appalachian State University
in partial fulfillment of the requirements for the degree of
MASTER OF SCIENCE

August 2015
Department of Sustainable Technology and the Built Environment

REDUCTION IN THERMAL RESISTANCE OF RESIDENTIAL WALL ASSEMBLIES BASED ON SIZE AND DISTRIBUTION OF VOIDS IN TWO TYPES OF INSULATION

A Thesis
by
HELEN WHISTLER BURKETT
August 2015

APPROVED BY:

Jeffrey E Ramsdell
Chairperson, Thesis Committee

Susan C. Doll
Member, Thesis Committee

Brian W. Raichle
Member, Thesis Committee

R. Chadwick Everhart
Chairperson, Department of Sustainable Technology and the Built Environment

Max C. Poole, Ph.D.
Dean, Cratis D. Williams School of Graduate Studies

Abstract

REDUCTION IN THERMAL RESISTANCE OF RESIDENTIAL WALL ASSEMBLIES BASED ON SIZE AND DISTRIBUTION OF VOIDS IN TWO TYPES OF INSULATION

Helen Whistler Burkett
B.A., Hendrix College
M.S., Appalachian State University

Chairperson: Jeffrey E Ramsdell

The performance of residential wall insulation is a major factor in a home's energy consumption. Despite improved materials and best practices, poor installation of wall insulation continues to be a significant problem in the residential construction industry. Efforts have been made to grade the quality of this installation. While this method considers the percentage of insulation missing or compressed, it does not account for the location or distribution of the insulation voids. This study empirically examines the effect of size, location, and distribution of voids in sample residential wall assemblies using fiberglass batts and dense pack cellulose insulation. These tests are performed using a calibrated hot box apparatus. The development, calibration, and characterization of the hot box is also examined in this study.

Acknowledgments

I would like to express my sincere gratitude to my advisor Dr. Jeff Ramsdell for his guidance throughout my graduate studies and his mentorship during my research assistantship at the Appalachian Energy Center. I would also like to thank my thesis committee members, Dr. Susan Doll and Dr. Brian Raichle for their insight and encouragement. I am grateful for the support of Dr. Marie Hoepfl as well.

Table of Contents

Abstract iv

Acknowledgments v

Chapter 1: Introduction 1

Statement of the Problem 1

Purpose of the Study 2

Research Questions 3

Limitations of the Study 4

Significance of the Study 4

Chapter 2: Review Of Literature 6

Residential Energy Use 6

Residential Insulation 7

Laboratory testing of thermal performance 7

Residential energy services network 7

Installation defects 8

Materials 9

Chapter 3: Research Methods 13

The Hot Box 13

Data collection procedure 13

Calibration procedure 19
Heat balance of hot box 20
Wall Sample 27
Insulation Void Configuration 28
Installation and Testing 32
Test Procedure 36
Chapter 4: Findings and Discussion 37
Calibration Test Series Results 37
Estimated R-Value of Tested Wall Samples 41
Wall Sample Test Results 41
Extraneous Heat Transfer 48
Temperature Distribution 50
Chapter 5: Conclusions 55
Research Questions 55
Future Work 56
References 58
Appendix A 63
Appendix B 68
Appendix C 71

Appendix D 74

Vita 76

Chapter 1: Introduction

According to the United States Department of Energy (USDOE), building energy consumption accounts for about 41% of the total energy consumption in the United States (United States Department of Energy [USDOE], 2012a, para. 8). As one of many efforts to reduce building energy use, codes and standards have been developed requiring minimum quality levels regarding the installation of residential wall insulation. The purpose of this study is to provide a controlled comparison of the reduction of thermal resistance due to gaps of increasing size in two common types of residential insulation, as well as to compare the effects of concentrated and distributed gaps. This study attempts to illustrate the impact of good workmanship for each type of insulation.

Statement of the Problem

The 2012 International Energy Conservation Code (IECC) requires insulation in residential wood frame walls that has an R-value of 13 to 20 $ft^2 \cdot °F \cdot hr/Btu$, depending on climate zone (International Energy Conservation Code [IECC], 2012, sec. R402.1). Although manufacturers produce insulation that is laboratory tested to meet these standards, the installed insulation is, at most, inspected visually. Harley found, “In practice, manufacturers’ instruction and industry standards are widely ignored; insulation is often installed with substantial defects. Insulation installers and others who have a stake in the work...do not understand the performance implications of these defects” (Harley, 2007, Abstract, para. 2).

At its core, the problem is the discrepancy between the rated thermal resistance of laboratory tested insulation and the actual thermal performance of in-situ wall assemblies (Brown, Bomberg, Ullett, & Rasmussen, 1993; Cammerer, Spitzner, Treiber, Schmitt, & Heinz, 2003; Lawton, Roppel, Fookes, St. Hilaire, & Schoonhoven, n.d.; Straube, 2007; Threthowen, 1991). Because of the pervasiveness of installation defects in insulated residential wall assemblies, the industry must understand the degree to which the voids decrease the thermal resistance of the wall. The effect of voids of equal size may not be the same for all insulation materials.

The IECC does not dictate a type of insulation used in residential wall assemblies; consequently, we must understand the effect of insulation voids in different types of insulation. There have been many studies using laboratory tests or energy modeling to quantify the effect of poor workmanship on insulation effectiveness. Several materials have been examined, including mineral fiber (Brown et al., 1993), fiberglass batts (Christian & Kosney, 1998), extruded polystyrene boards (Trethowen, 1991), and others. However, no controlled studies have been found that examine the relationship between the size of gaps and reduction of thermal resistance across different types of insulation. Given the different installation methods used and the advancements in insulation products since these studies were conducted, the industry needs more than a synthesis of the existing results.

Purpose of the Study

In order to understand the effect of voids and poor installation, this study undertakes a side-by-side comparison of fiberglass batts and blown-in cellulose, two commonly used types

of residential wall insulation, using the same testing conditions and equal size and locations of voids.

Residential Energy Services Network (RESNET) created a grading scale for the condition and completeness of installed insulation. This grading scale is used in many building codes and green building certifications. Grades are determined by the percentage of insulation missing and the percentage of insulation compressed. These percentages are the same regardless of the insulation material or the location or concentration of the voids. This assumes that insulation voids have the same effect on thermal resistance of all types of materials. This study examines that assumption.

Research Questions

1. In standard residential construction, how do voids in different types of wall insulation affect the total thermal resistance of the wall assembly?
2. What is the correlation between the size of the void, as a percentage of the total insulated area, and the magnitude of the reduction in thermal resistance? Is there a difference in this correlation between two widely used residential insulation materials?
3. How does the distribution of voids affect total R-value? For example, does a 2% void concentrated in one place affect the total R-value differently than smaller voids that add up to 2% distributed across the sample? Or, do voids of the same size, but different locations and orientations affect the total R-value differently?

Limitations of the Study

Although only two types of insulation are examined, the procedure established in this study could be applied to other types of insulation and to other types of assemblies, such as attics and floors. The number of tests performed is constrained because of the lengthy duration (6-12 hours) of each test. The sample walls reflect typical residential frame construction, but do not simulate heat flow through connections with a ceiling, floor, or adjacent walls. This may, as Christian and Kosny (1997) show, result in higher clear wall R-value than the more realistic whole wall R-value (see *Installation defects* section). However, since all materials are tested in the same manner, this should have little effect on their comparison.

Significance of the Study

This study seeks to determine what effect insulation voids have on overall wall thermal resistance, and whether or not that effect is the same in different types of insulation. This information will add to the body of knowledge concerning residential insulation, and it will assist builders and homeowners in decisions about what type insulation to use. An understanding that poor workmanship in the installation of one type of insulation may have a greater detrimental effect on the building's energy use will be valuable to industry professionals. Along with an assessment of the cost of materials, cost of installation, and resulting energy use, this understanding will inform industry professionals when choosing which type of insulation to use and how much attention to installation detail is justified.

The sample insulation materials and the design of the wall assembly were chosen to represent an average production-built home. There are two reasons for this focus. First,

production-built, light-frame homes are known to have significant insulation defects (Harley 2007; Harvey, 2006). Second, these homes offer the most energy saving potential, because addressing the problems in production homes that are merely “built to code” will affect a greater share of the building stock than reducing the energy use of homes that incorporate advanced insulation products and sustainable design.

Chapter 2: Review of Literature

Residential Energy Use

In an industry moving toward more sustainable practices, researchers and builders are faced with many options of products and methods that improve energy efficiency. Space heating and cooling makes up the majority of residential energy consumption. This consumption can be reduced with improved HVAC equipment and distribution systems, and an effective building envelope that minimizes heat loss or gain. M.S. al-Homoud explains,

> The amount of energy required to cool/heat a building depends on how well the envelope of that building is treated thermally, especially in envelope-dominated structures such as residences. The thermal performance of [the] building envelope is determined by the thermal properties of the materials used in its construction. (al-Homoud, 2004, p. 353)

There are many elements of the building envelope that affect its integrity. The building envelope must consist of an air barrier, a vapor barrier, and a thermal barrier. Air infiltration or exfiltration replaces the conditioned air with outside air that reduces the indoor comfort and requires more energy to maintain the desired temperature. The vapor barrier, or retarder, reduces the rate of moisture transfer through the building assembly to prevent condensation in or on the building materials. The thermal barrier slows the transfer of heat through the building assembly, which reduces the amount of energy used to maintain the desired indoor temperature. While proper management of air and moisture is integral to an efficient and long lasting home, this study focuses on the thermal barrier and the insulation that constitutes it.

Residential Insulation

Laboratory testing of thermal performance. Starting with the introduction of the R-value measurement system in 1945, many insulation testing methods have been developed, each with their own apparatus. ASTM, formerly known as the American Society for Testing and Materials, has created standard testing methods for the guarded-hot-plate, heat flow meter, thin-heater, guarded hot box, and calibrated hot box apparatuses. The advantage of the guarded and calibrated hot box apparatuses is their ability to test whole wall assemblies, rather than a single material. Hot boxes can also accommodate large samples, typically 4'x8', and in the case of Oak Ridge National Laboratory's guarded hot box, as large as 10'x 13' (Oak Ridge National Laboratory [ORNL], 2004, para. 2). Because these measurements are made under controlled laboratory conditions, a common criticism is that they do not accurately represent thermal performance in the field: "Insulation materials are usually characterized by material tests which do not necessarily resemble the actual material properties in the wall" (Cammerer et al., 2003, p. 1).

Residential energy services network. RESNET is an organization that sets standards for residential building energy efficiency (Residential Energy Services Network [RESNET], 2014, sec. 1). In addition to the building industry, these standards are recognized by federal agencies such as "IRS for tax credit qualifications, U.S. Environmental Protection Agency for ENERGY STAR labeled homes, [and] U.S. Department of Energy for Building America and National Builders Challenge programs" (RESNET, 2014, sec.2). In 2006, RESNET introduced a procedure for degrading wall R-value (Figure 1) according to installation quality (Harley, 2007, p.2).

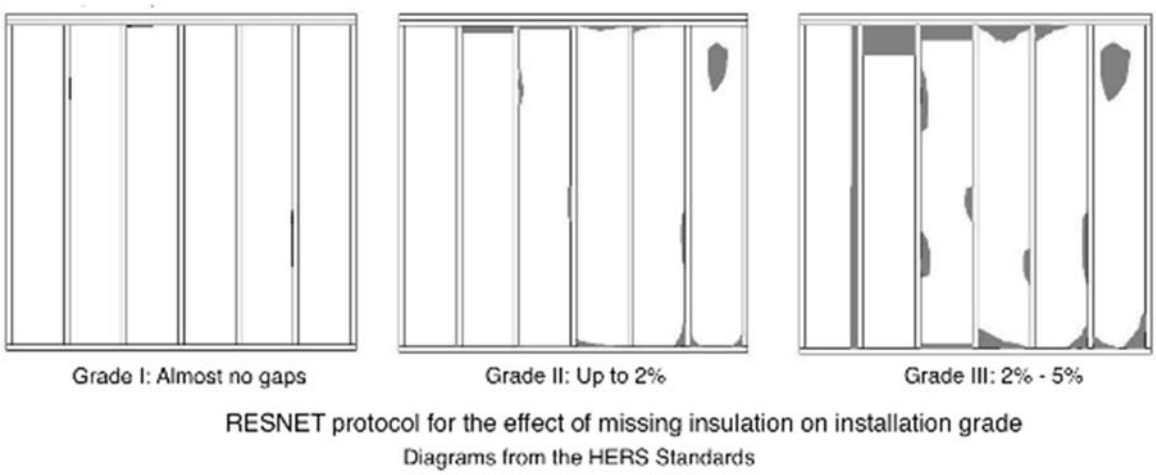

Figure 1. RESNET categories for installation quality (Green Building Advisor, 2012, image 3).

Installation defects. The effectiveness of insulation's thermal resistance can be reduced due to age deterioration, air and moisture movements, and improper installation. As John Straub explains, the relationship between the material and its installation is important:

> If insulation is improperly installed, or if a product is installed in an improperly designed enclosure system, the performance of the complete enclosure can be very different than that of the product. In some cases the R-value labeled on a product will control the flow of heat with 1/2 or 1/3 the level expected by many professional specifiers and consumers. (Straube, 2009, p. 2)

In addition to wasted energy, there are other problems caused by gaps in insulation: "Gaps within the insulation would lead to an increased local heat loss (which in itself is not acceptable) and possibly to low surface temperature. The latter could cause water vapour [*sic*] condensation and lead to mould [*sic*] growth" (Cammerer et al., 2003, p. 1). This moisture can further reduce the thermal resistance by saturating the fibrous materials (Bynum, 2001, p. 37).

Trethowen (1991) finds, in his study of workmanship in extruded polystyrene wall insulation, that "there is no tolerance for workmanship imperfection" (p. 177). Defects in insulation have a significant effect on the thermal resistance of the wall assembly. Despite a proven relationship between improper insulation installation and reduced thermal resistance, poor workmanship continues to be a problem. Unfortunately, as Harley states, "insulation is difficult to install perfectly - and in most markets, with installers paid by the ft^2, there's little incentive to get the details right" (Harley, 2005, p. 20). Common workmanship problems associated with each type of insulation are discussed in the following section.

Researchers have studied the effectiveness of thermal insulation with regard to improper installation as well as to proper installation in wall assemblies that more accurately represent typical construction. Christian and Kosney established three types of measurements for thermal resistance of wall assemblies. The Center-of-Cavity R-value is the thermal resistance of the wall assembly without the studs. The Clear-Wall R-value is the thermal resistance of the wall assembly with studs. The Whole-Wall R-value is the thermal resistance of the wall assembly with studs and "typical envelop interface details. These details include wall/wall (corner), wall/roof, wall/floor, wall/door, and wall/window connections" (Christian & Kosny, 1997, p.16). This study will determine clear-wall R-values.

Materials. Countless materials have been used as thermal insulation, from straw bales to vacuum-insulated panels. As Karamanos et al. describe, "The common feature in all insulation materials is their low thermal conductivity factor λ, usually lower than .01 W/mK. This owes to the fact that a quantity of gas, usually air, is embodied in the material's mass" (Karamanos, Papadopoulos, & Anastaselo, 2004, p.1). For this study, the focus on insulation materials commonly used for residential wall applications. Three such materials are kraft-

faced fiberglass batts, loose fill or blown-in cellulose, and polyurethane spray foam insulation (Jelle, 2011). The most common material used in residential application is fiberglass, comprising 53% of market demand, followed by foamed plastic (which includes polyurethane spray foam) at 26% and cellulose at 10% (USDOE, 2012a, Sec. 5.1.1). In the following sections, these materials are described in terms of installation, thermal resistance properties, and the factors affecting their effectiveness.

Fiberglass batt insulation. Fiberglass batts are comprised of glass that has been melted and spun into threads (Bynum, 2001, p. 120). The batts can be faced with kraft paper on one side, to act as a vapor retarder, or be unfaced. Importantly, fiberglass is not an air barrier. The thermal conductivity varies by manufacturer, but properly installed fiberglass batts have a thermal conductivity of 0.04-0.033 W/m/K (al-Homoud, 2004, p.362).

While fiberglass batt insulation is relatively inexpensive, it is best "suited for standard stud and joist spacing that is relatively free from obstructions" (USDOE, 2012b, table 1). Installation is more difficult around obstructions or in odd sized stud bays. Improper installation in such applications can cause compression, which reduces the overall thermal resistance of the material (Bynum, 2001, p. 127). A study by the California Energy Commission examined the installation of batt insulation in 30 new so-called energy efficient houses. They found that 40-60% of houses were observed to have "stuffing of insulation in non-standard width cavities" (Harvey, 2006, p. 44). They also found that 100% of the houses demonstrated "a failure to cut the insulation (rather than compressing it) to fit around wiring, plumbing, and electrical boxes" (Harvey, 2006, p. 45). In fiberglass batts, "air gaps often form at the corners of batt insulation because of defects in installation. This common defect

can allow significantly more heat flow than the rated R-value would suggest as it allows convective loops to form" (Straube, 2009, p.14).

Blown-in cellulose. Cellulose insulation is made of recycled pulp from paper products such as newsprint, and treated to be fire resistant (Bynum, 2001, p. 80). Blown-in cellulose is installed by first attaching netting to the framing members to serve as a retainer for the blown-in cellulose during installation. A pneumatic blowing machine is used to install the insulation. Blown-in cellulose can be installed at different densities; these are referred to as loose-fill or dense-pack. The installation process is similar, although dense pack requires more precise equipment and installation practices in order to ensure an even and accurate density. Loose-fill is more common in attics, but is also used in walls. Unlike fiberglass batts, blown-in cellulose is well suited for odd-sized cavities or around obstructions. However, in their study on the settling of cellulose insulation, Cammerer et al. (2003) explain, "settling of loose-fill insulation in walls may occur due to bad workmanship or low density of the filling" (p. 1). As a result, voids can form "at the top of wall cavities, above windows, [and] around doors" (Bynum, 2001, p.79). A study on gaps in loose-fill insulation indicates a severe reduction in thermal resistance due to gaps as small as 49 cm^2 (Cammerer et al., 2003). The thermal conductivity varies by manufacturer, but properly installed to the correct density, blown-in cellulose has a thermal conductivity of 0.054-0.046 W/m/K (al-Homoud, 2004, p.362). Dense pack insulation faces similar issues of poor workmanship, as Baum found in his study on the installation quality dense-pack cellulose insulation (Baum, 2010, slides 37-49). His research showed that wall samples with realistic obstructions such as wiring and bracing "had measured densities of 33% and 29% below what is considered adequate for dense packing" (Baum, 2010, slide 47).

Polyurethane spray foam. Polyurethane spray foam is a fundamentally different type of insulation. It is a two-part foam which is combined on site as part of the installation process. The mixing of the two chemicals creates "millions of tiny closed plastic cells filled with an inert gas. The inert gas resists heat transfer better than regular air" (Bynum, 2001, p.193). Unlike fiberglass, spray foam insulation "serves as an air barrier (thus reducing infiltration as well as conductive heat losses)" (Harvey, 2006, p. 46). Polyurethane spray foam has a thermal conductivity of .023 W/m-K (al-Homoud, 2004, p.363).

Although spray foam insulation works well around obstructions and in odd-sized wall cavities (Harvey, 2006, p.46), it is nonetheless susceptible to poor workmanship defects. "When components are poorly mixed, or mixed in the wrong ratio or at the wrong temperature, cured foam has been known to shrink away from rafters or studs, leaving cracks. Some installers rush through their spraying, resulting in voids" (Green Building Advisor, 2013, para. 7).

Chapter 3: Research Methods

This study used an experimental approach to gather empirical data measuring the thermal resistance of sample wall assemblies with varying amounts of insulation missing. The size of the voids were determined using RESNET's grading scale as a guide (Green Building Advisor, 2012). The effect of distribution of gaps was also examined by testing the thermal resistance of a wall with a concentrated horizontal insulation void, a wall with a concentrated vertical insulation void, and a wall with six distributed voids that comprise an equivalent total area.

The Hot Box

A calibrated hot box was used to measure total thermal resistance for each wall assembly. The hot box apparatus is comprised of two small rooms measuring 11′ x 3′ and 8′ tall, separated by a wall that holds a 4′x8′ wall assembly to be tested as shown in Figure 2. Each room is either heated or cooled to given set points. Thermal transmittance is determined by measuring the amount of additional energy required to keep the hot side at the set point. The majority of this heat is flowing through the sample to the cold side. After calibrating for losses from the apparatus itself, the amount of heat flowing through the wall sample to the cold side is determined. The apparatus was calibrated by performing tests on identical materials with known R-values. The calibration tests used extruded polystyrene boards of three thicknesses. These calibration tests were performed in order to derive a correction factor based on the percent error between the test results and the known R-values. This correction factor was then applied to the results of the wall sample tests.

The two sides were conditioned to produce a temperature differential of 40° Fahrenheit. The cold side was cooled using a 12,000 Btu/hr window air-conditioning unit controlled with a CoolBot™ controller (Store It Cold, North Fort Myers, FL), which overrides the built in set point of the air conditioner. A baffle was installed to direct the cold air across the chamber, rather than directly at the sample. An 800 W electric resistance heater with a built in fan was used to heat the hot side. A baffle above and to the side of the heater reduced localized radiant heat transfer to the sample. Both the cooling unit and the heater were controlled by external thermostats, rather that the built-in thermostats, in order to increase the precision of the set points. The energy supplied to the heater to keep the hot side at the set point is measured by a Watts up?® power meter (ThinkTank Energy Products Inc., Milton, VT). This meter logs kWh used throughout the test, which is used to calculate the thermal resistance of the sample wall. Figure 2 illustrates the general layout of the hot box and the heating and cooling equipment.

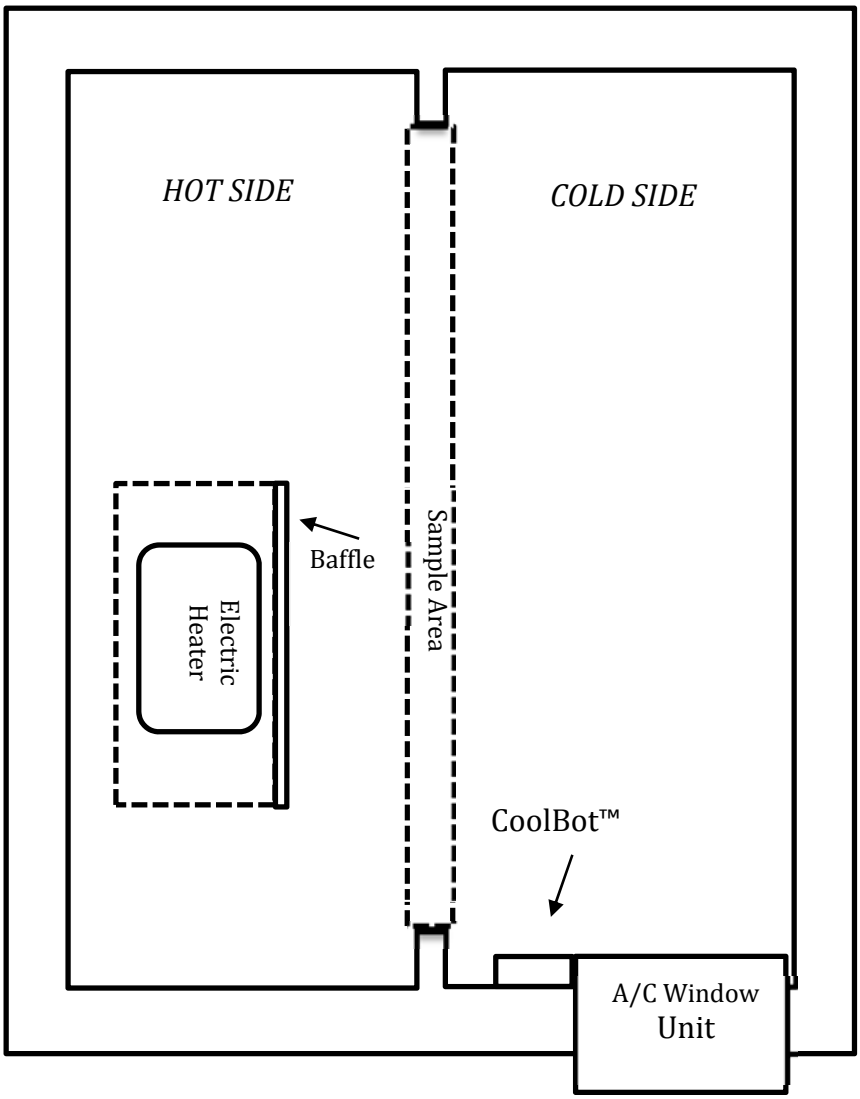

Figure 2. Hot box apparatus diagram (NTS)

The hot box is equipped with DS18B20 thermal sensors (Maxim Integrated, San Jose, CA) to provide temperature readings on the sample surface and throughout the hot box volume with an accuracy of ±0.5°C from -10°C to 85°C. The sensors have a digital signature, which allows them to be wired in series, rather than parallel, and results in no loss of resolution during the data collection process. The data acquisition system for the hot box was designed as a star configuration, using five CAT5 cables with up to 24 sensors in series.

These sensors are connected to an Arduino Uno® board (Arduino, Somerville, MA) which both powers the sensors and gathers temperature data from the sensors to log in an Excel file. There are a total of 104 sensors: 20 on each surface of the sample, 24 hanging in a grid in each chamber, 8 on the interior surface of the wall between the hot chamber and ambient air, and 8 on the exterior surface this wall Figure 3 is a cutaway schematic of the sensor layout in the hot chamber. The white cubes are the 24 sensors suspended from the ceiling; the black cubes are the 20 sensors attached to the surface of the sample. The sensors in the cold chamber are arranged in an identical manner, so that the sensors are aligned with each other.

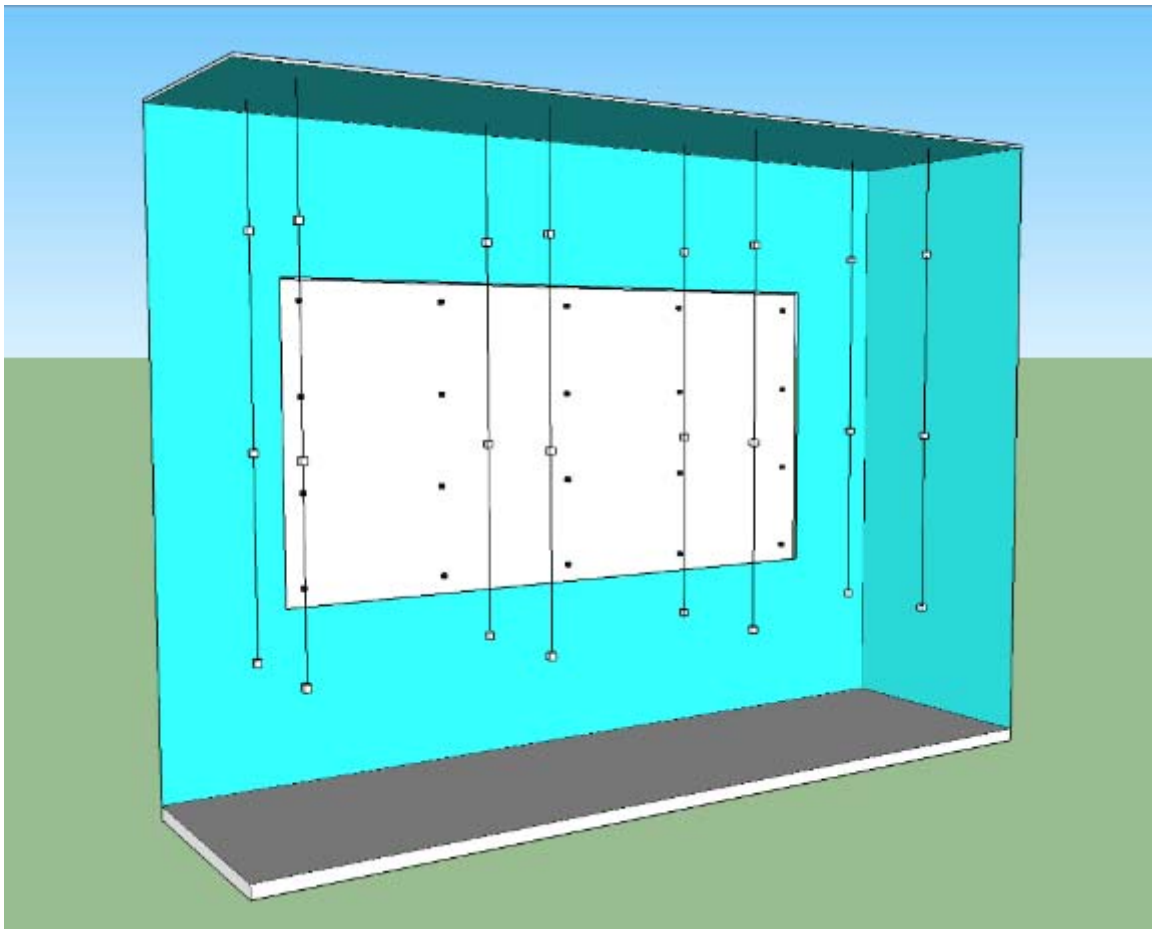

Figure 3. Hot box sensor location schematic

Figures 4 through 8 show the sensor wiring process, the location of the sensors, and the interface with the Arduino board.

Figure 4. Connecting three wires in series

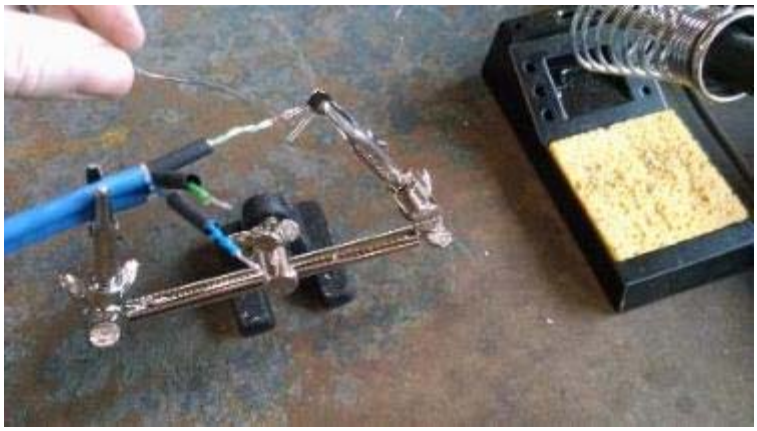

Figure 5. Soldering wires to DS18B20 terminals

Figure 6. Protecting connections with heat shrink tubing

Figure 7. Sensors on sample and in hot side chamber (not pictured: sensors on interior surface of chamber wall)

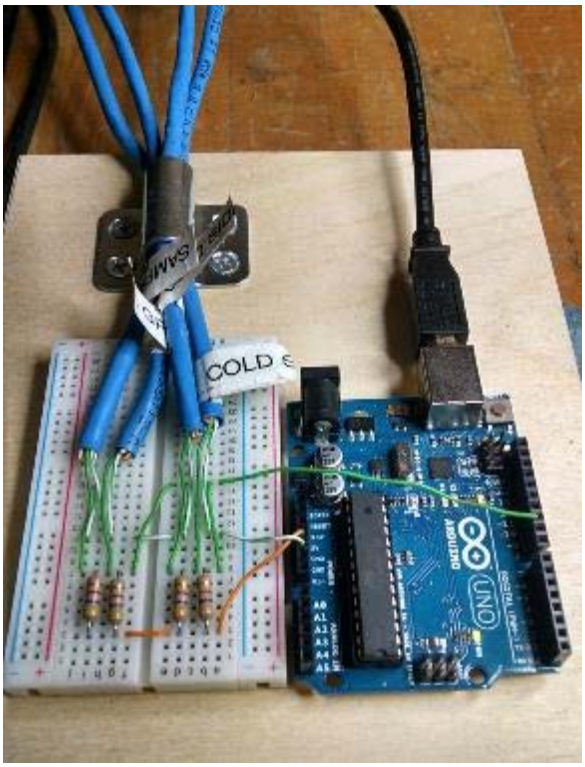

Figure 8. Arduino and breadboard connections

Data collection procedure. The testing was conducted using the ASTM C1363-05: Standard Test Method for Thermal Performance of Building Materials and Envelope Assemblies by Means of a Hot Box Apparatus (ASTM International, 2005) as a guide. While the overall procedure, including specimen orientation, sample sealing, energy metering, and temperature measurement of sample, airspace and metering wall were maintained, meeting all the requirements of the standard was not feasible given the resources and testing equipment available for this study. Some specifications such as "a means for determining air

velocity past both the hot and cold faces of the specimen during each test" (ASTM, 2005, p.12) were not included because appropriate equipment was not available.

The method for determining the hot box operating temperatures is specified in ASTM C1058. This standard recommends "that thermal properties of insulation materials be evaluated over a mean temperature range that represents the intended end use" (ASTM, 2010, p. 2). It offers the temperature differentials in Table 1.

Table 1. ASTM Recommended Temperatures (ASTM, 2005, p.3)

Hot Side (°F)	Cold Side(° F)
75 ± 9	5 ±9
100 ± 9	50 ± 9
145 ± 9	75 ±9

In order to limit heat transfer through the exterior hot box walls, the hot side was kept at a temperature close to room temperature. The cold side was kept as cold as possible with the available equipment. The chosen thermostatic set points (77°F for the hot side and 37°F for the cold side) are within a normal range of indoor and outdoor temperatures during a heating season.

Calibration procedure. The hot box was calibrated through a series of tests of extruded polystyrene insulation with known R-values. Dow® STYROFOAM™ Brand Residential Sheathing (The Dow Chemical Company, Midland, MI) were used in ½″, ¾″, and 1″ dimensions, with thermal resistance of R-3, R-3.8, and, R-5.0 $ft^2 \cdot °F \cdot hr/Btu$ respectively. Three individual sheets, 4′ x 8′ in size, of each thickness were used, resulting in

nine distinct samples tested. Each sample was caulked to the surround (i.e., the 10″ deep insulated frame around the sample opening) to prevent air leakage around the sample. Thermal conductive paste was used to ensure thermal contact between the sensors and the sample, and Gorilla Tape® (The Gorilla Glue Company, Cincinnati, OH) was used to secure the sensors and the Cat5 cables in place.

Between each test, the heating and cooling equipment was turned off. The sensors were removed from both the hot and cold sides of the sample. The sample was removed, and residual caulk was removed from the surround. Each sample was marked A, B, or C to identify it in relation to the results of the test. The next sample was installed, and the sensor placement was measured and marked in the arrangement shown in Figure 3. The sensors were re-attached in the same manner as previously described. The heating and cooling equipment was then turned on, and the doors to each chamber were closed. The datalogging program was activated, and the real-time data was monitored. The time it took for each chamber to reach thermal equilibrium depended on a number of factors, including the ambient temperature and the R-value of the sample. Typically, this would take around four hours, and was determined visually. The tests were continued overnight, gathering approximately 12 hours of steady-state data.

Heat balance of hot box. In addition to the intended heat transfer through the tested sample, there are three additional paths of heat transfer that must be considered in the heat balance of the hot box. These are through the exterior wall, floor and ceiling of the hot-side chamber to ambient, the wall separating the hot and cold chambers, and the flanking path within the frame around the sample. The hot box is designed so that these components have a much higher resistance to heat transfer than the sample. However, this additional heat

transfer cannot be completely eliminated and therefore, it must be calculated in order to subtract it from the measured total energy (Q). The resulting net Q is the heat transfer through the sample itself.

First, the hot box exterior walls, floor, and ceiling have a high R-value. However, because the ambient temperature cannot be maintained at the hot-side temperature, as it would be in a guarded hotbox, there will be some heat loss through the exterior walls of the hot chamber of the hot box. Metering box wall loss, or the heat flow through the hotbox walls rather than through the sample is calculated using Equation 1.

$$Q_{mw} = \frac{A_{in} * (t_{in} - t_{out})}{R}$$

Where:

Q_{mw} = Heat transfer rate through metering walls (and floor and ceiling)

A_{in} =metering chamber inside surface area

t_{in} = metering chamber inside wall surface temperature

t_{out} = metering chamber outside wall surface temperature

R= RSI of metering walls, ceiling and floor

Equation 1. Equation and definitions for estimating metering box wall loss.

The combined RSI of the walls, ceiling and floor of the metering box was calculated using a weighted average of the RSI of each assembly. Using known materials and thicknesses, the RSI of each assembly was determined by a parallel path calculation, as shown in Tables 2 through 4. This method calculates the R-value of the path through studs separately from the path through insulation. Thus, the framing and insulation columns show identical R-values for all layers of the walls, except for the framing and insulation layer. An

appropriate framing factor (i.e., the percentage of wall that is composed of studs or other framing) is then applied to each R-value. The estimated framing factor for the walls is 25% and the estimated framing factor for the ceiling and floor is 11%. Taking a weighted average of these three RSI values with the ceiling and the floor each comprising 16% of total metering box surface area and the walls comprising the remaining 68%, the resulting RSI is 5.59. The estimated framing factors contributes the greatest uncertainty to the calculated dividing wall RSI value. This uncertainty is estimated to be 9%.

Table 2. RSI Parallel path calculation of metering box walls

Metering box walls	R-value ($ft^2 \cdot °F \cdot hr/Btu$)		
	Framing	**Insulation**	
Exterior air film*	0.68	0.68	
OSB	0.62	0.62	
XPS	3	3	
Cavity insulation		20.35	
Cavity framing	6.88		
XPS	10	10	
Interior air film	0.68	0.68	
Total R-value	21.855	35.33	
% of Wall	25.0%	75.0%	
% / R	0.0114	0.0212	
Sum %/R (U-factor of wall)			0.0327
R-value (1/U) ($ft^2 \cdot °F \cdot hr/Btu$)			**30.61**
		RSI ($m^2 \cdot K/W$)	**5.39**

*Using interior air film R-value because exterior of metering box is conditioned space

Table 3. RSI Parallel path calculation of metering box ceiling

Metering box ceiling	R-value ($ft^2 \cdot °F \cdot hr/Btu$)		
	Framing	**Insulation**	
Exterior air film*	0.68	0.68	
OSB	0.93	0.93	
XPS	3.8	3.8	
Cavity insulation		28.13	
Cavity framing	6.88		
XPS	10	10	
Interior air film	0.68	0.68	
Total R-value	22.965	44.215	
% of Wall	11.0%	89.0%	
% / R	0.0048	0.0201	
Sum %/R (U-factor of wall)			0.0249
R-value (1/U) ($ft^2 \cdot °F \cdot hr/Btu$)			**40.13**
		RSI ($m^2 \cdot K/W$)	**7.07**

*Using interior air film R-value because exterior of metering box is conditioned space

Table 4. RSI Parallel path calculation of metering box floor

Metering box floor	R-value ($ft^2 \cdot °F \cdot hr/Btu$)		
	Framing	**Insulation**	
Exterior air film*	0	0	
OSB	0.93	0.93	
Cavity insulation		34.38	
Cavity framing	6.88		
OSB	0.93	0.93	
Interior air film	0.68	0.68	
Total R-value	9.415	36.915	
% of Wall	11.0%	89.0%	
% / R	0.0117	0.0241	
Sum %/R (U-factor of wall)			0.0358
R-value (1/U) ($ft^2 \cdot °F \cdot hr/Btu$)			**27.94**
		RSI ($m^2 \cdot K/W$)	**4.92**

*No exterior air film

Table 5. Weighted average of metered walls, ceiling, and floor

Component	**RSI ($m^2 \cdot K/W$)**	**% Area**
Walls	5.39	68%
Ceiling	7.07	16%
Floor	4.92	16%
Total	**5.59**	

The second additional path of heat transfer in the hot box is through the wall separating the hot and cold chambers. This is similarly calculated using Equation 2. Again the RSI of the dividing wall is determined using a parallel path calculation shown in Table 6.

$$Q_{dw} = \frac{A_{dw} * (t_{env,h} - t_{env,c})}{R}$$

Where:

Q_{dw} = Heat transfer through dividing wall between the hot and cold chambers

A_{dw} = Net area of dividing wall, not including sample area

$t_{env,h}$= air temperature inside hot chamber

$t_{env,c}$= air temperature inside cold chamber

R= RSI of dividing wall between hot and cold chambers

Equation 2. Equation and definitions for heat transfer through the wall dividing the hot and cold chambers

Table 6. RSI Parallel path calculation of dividing wall

Dividing wall	R-value ($ft^2 \cdot °F \cdot hr/Btu$)		
	Framing	**Insulation**	
Exterior air film	0.68	0.68	
housewrap			
XPS	10	10	
Cavity insulation		21.00	
Cavity framing	6.88		
OSB	0.62	0.62	
XPS	10	10	
Interior air film	0.68	0.68	
Total R-value	28.855	42.98	
% of Wall	11.0%	89.0%	
% / R	0.0038	0.0207	
Sum %/R (U-factor of wall)			0.0245
R-value (1/U) ($ft^2 \cdot °F \cdot hr/Btu$)			**40.78**
		RSI ($m^2 \cdot K/W$)	**7.18**

The third additional path of heat transfer is the flanking loss around the sample, through the frame of the surround. This is different from the dividing wall loss in that it is not a one-dimensional heat transfer. Figure 9 shows a schematic of flanking loss as well as metering box loss. (Note that dividing wall loss is not included in this schematic because there is no dividing wall; the hot and cold chambers are only divided by the specimen itself. As Lavine, Rucker, and Wilkes show in their study, flanking loss is typically 6% of specimen heat transfer (Lavine, Rucker, and Wilkes, 1983, p. 247). The metered heater power when it was not running was between 2.2W and 2.5W. When the heater was running, the power readings were between 750 and 800W.

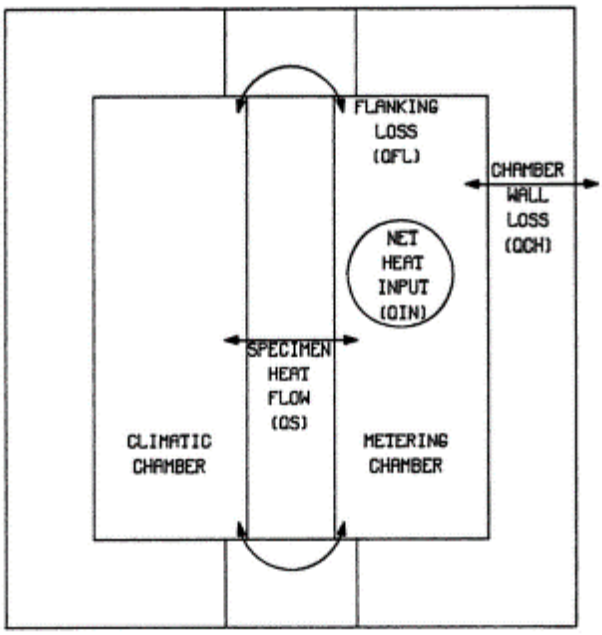

Figure 9. Schematic showing flanking loss around a sample (Lavine et al., 1983, p. 235)

R-value calculation. Using this information about the hot box construction and the temperature data measured throughout a test, the RSI of the sample was calculated using Equation 3.

$$R = \frac{A * (t_{env,h} - t_{env,c})}{(Q - Q_{mw} - Q_{dw}) * (1 - F)}$$

Where:

A= Area of sample

$t_{env,h}$= air temperature inside hot chamber

$t_{env,c}$= air temperature inside cold chamber

Q= Equilibrium power consumption of heater (without standby draw)

Q_{dw} = Heat transfer through dividing wall between the hot and cold chambers

Q_{mw} = Heat transfer rate through metering walls (and floor and ceiling)

F = flanking loss coefficient, estimated to be 6% of sample heat flow.

Equation 3. Overall R-value equation and definitions

Wall Sample

This study included 12 hot box tests of a 4′x8′ wall assembly sample. To simulate conventional residential construction, the most common residential building components were used. From interior (or hot side) to exterior (or cold side) the assembly was constructed as follows: ½″ drywall, 2″x 4″ nominal (1.5″x 3.5″ measured) softwood framing members 16″ on center, with insulation in stud bays, oriented strand board (OSB), and Majpell 5 vapor control layer as housewrap. Typically, this construction would include drywall compound and paint. These materials were excluded because of the additional application and drying time, as well as the difficulty to recreate an exact application for each test. These materials have little to no influence on the total thermal resistance of the wall, given that a full 4′ x 8′ drywall sheet was used, so there were no drywall joints. Figures 10 and 11 document the construction of the wall sample.

Figure 10. Framed wall sample

Figure 11. Insulation and drywall installed and sealed

Insulation Void Configuration

The wall assembly was first tested in the calibrated hot box with no insulation voids. After the test was completed and R-value calculated, the wall sample was opened by removing the drywall. Without compressing the surrounding insulation, 2% of the insulated area was removed, in one concentrated horizontal void, the full depth and width of the stud bay. This void measured 14 ½″ x 5 ¼″, or 75 ¼ in^2. The drywall was reattached and sealed to the sample surround with caulk, and the wall assembly was tested again. The 2% void was then increased to 5%. The 5% void measured 14 ½″ x 13″, or 188 ½ in^2. The thermal resistance of the wall assembly was tested again. Following this test, the stud bay containing the void is re-insulated to the original level, and tested. A vertical gap along the edge of the

stud bay is then removed, measuring 1 ¾″ x 44 ⅝″, or 75 ½ in^2, again accounting for 2% of the total insulation. After testing this configuration, the stud bay was reinsulated and six separate cylindrical voids, measuring 4″ in diameter, were distributed across the sample, each constituting 0.33% of total insulated area, totaling 2%. The thermal resistance of the wall assembly was tested again. The gaps were intentionally kept away from the edges of the sample area. Figures 12 through 16 illustrate the location and configuration of gaps for each test.

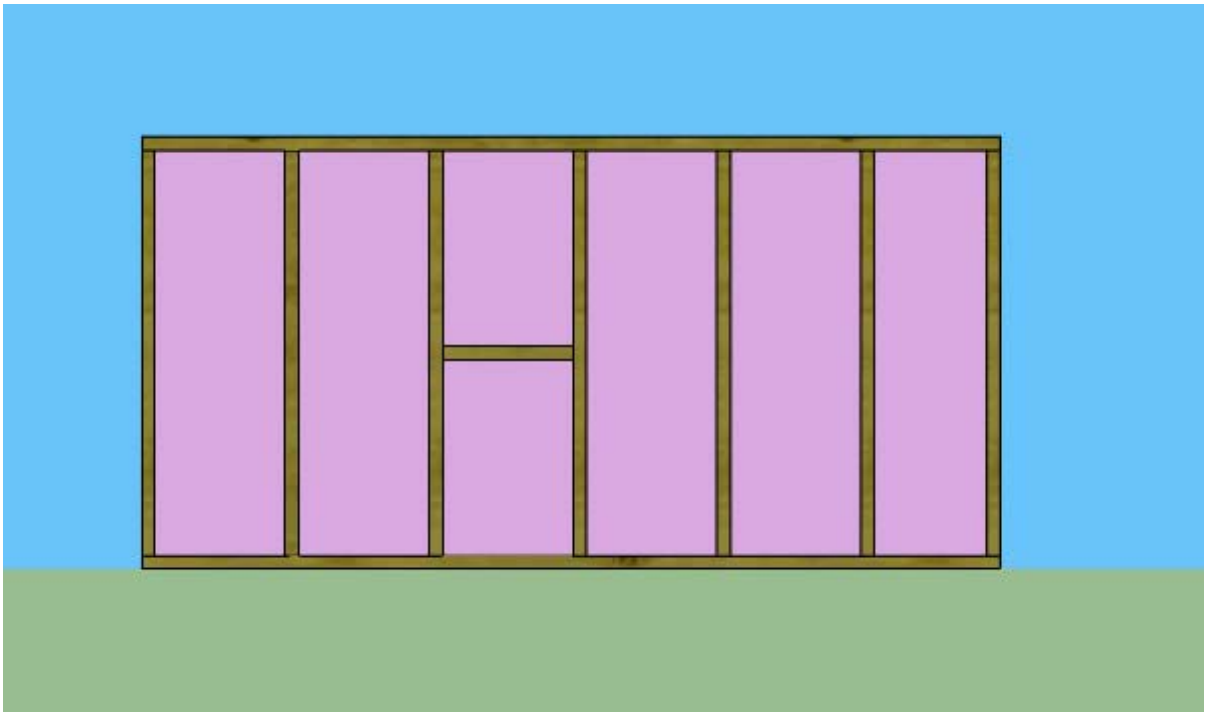

Figure 12. No voids

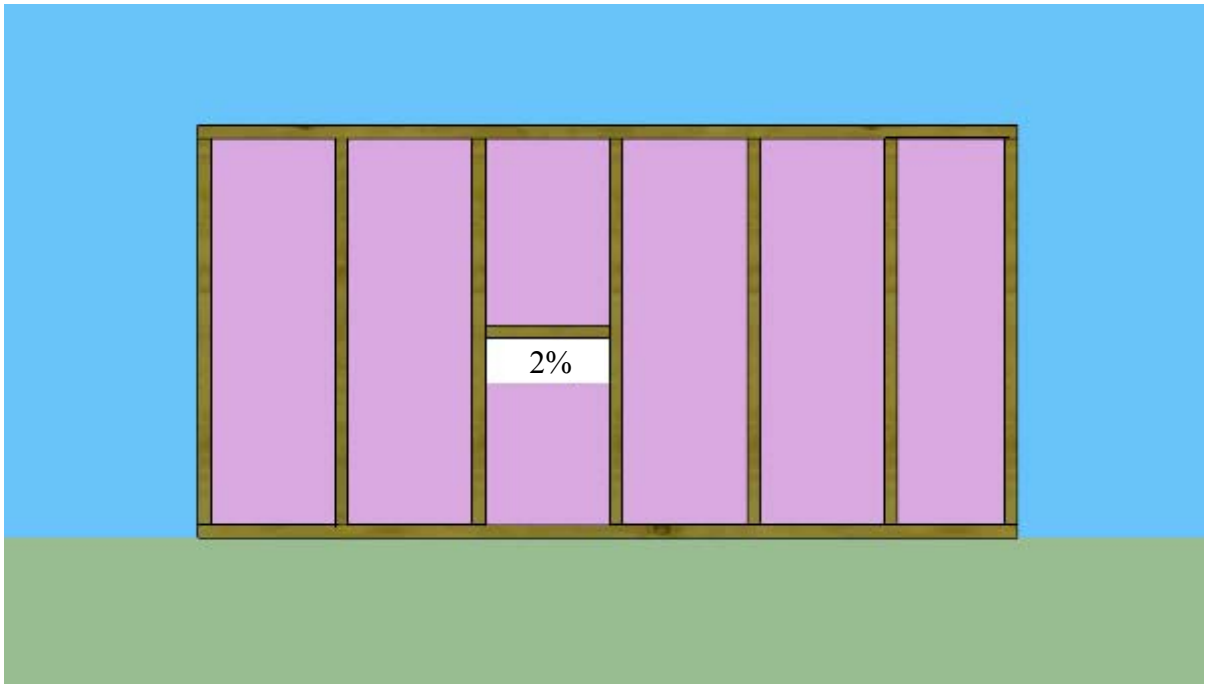

Figure 13. 2% horizontal void

Figure 14. 5% horizontal void

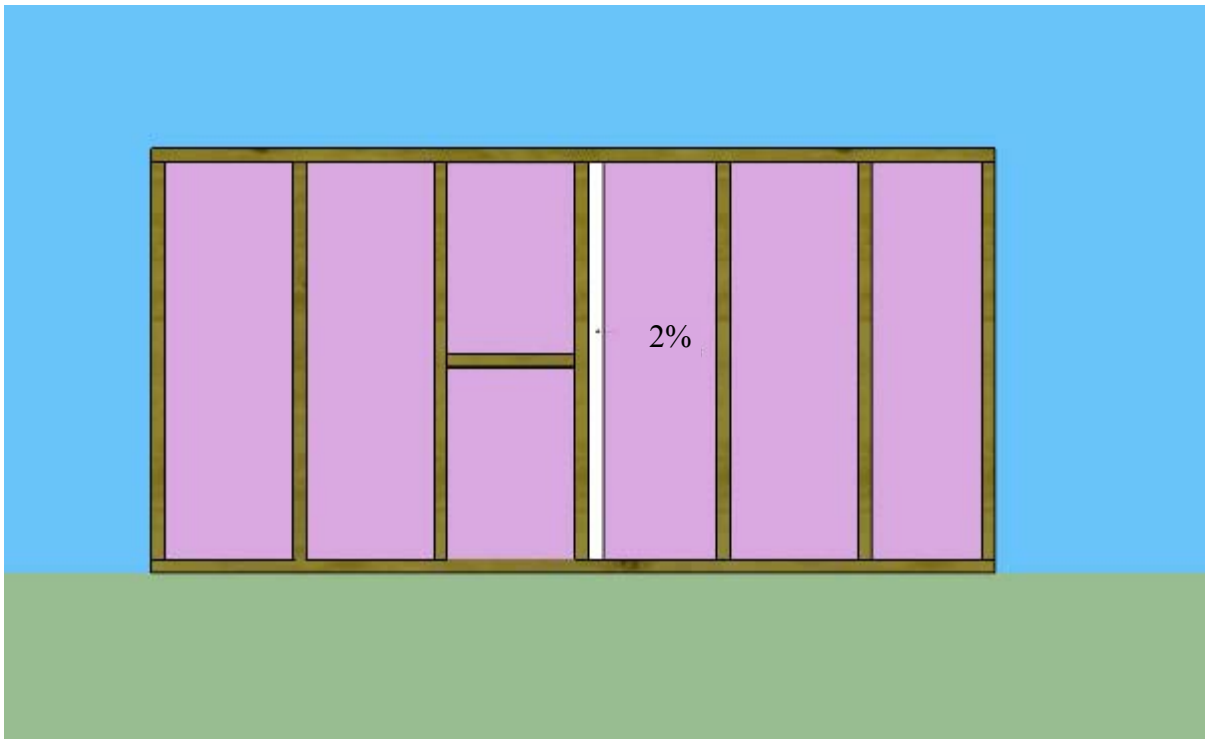

Figure 15. 2% vertical voids

Figure 16. 2% distributed voids

Installation and Testing

Fiberglass batts. The first series of six tests involved kraft-faced fiberglass batt insulation with a rated resistance value of R-15. Great care was taken to properly install both types of insulation according to manufacturer's specifications in order to create virtually no gaps as a baseline. CertainTeed® R-15 kraft-faced fiberglass batts (CertainTeed Corporation, Valley Forge, PA) were installed using the following instructions:

> Place the insulation between framing members and check to be sure it fits the cavity at both ends. With facing material flush with the face of the framing, the flanges will overlap the framing. Staple the flanges to the face of the framing every 8 in. or so. (CertainTeed Corporation, 2014, p.1)

Although the manufacturer also describes side (inset) stapling as an acceptable and widely used method, this method was not used due to its inherent susceptibility to gaps and compression. Batts were precisely measured and cut to ensure proper fit in stud bays, including the non-standard sized stud bay, measuring 12 ½″ wide. The process of removing portions of insulation was also carefully performed in order to take out the correct amount of insulation and to not damage or compress the surrounding insulation, as shown in Figures 17 through 19.

Figure 17. Measuring area of 2% horizontal void

Figure 18. Cutting holes for 2% distributed test

Figure 19. Distributed voids, totaling 2%

Dense pack cellulose. The second series of tests examined blown cellulose insulation. Cellulose was installed using the dense pack method described by Green Building Advisor (Kanarek & Dobsevage, 2015) and the density specifications from the manufacturer

(GreenFiber, 2013). Density was checked using the bag weight, bag count, and total insulated volume. Figures 20 and 21 show parts of the installation and removal process.

Figure 20. Wall sample with netting

Figure 21. Wall sample with 2% of cellulose removed

Based on the recommended density of 3.2 to 3.5 lbs./cu. ft. for dry dense pack cellulose, the sample wall required 26.16 lbs. of cellulose to obtain a density of 3.5lbs./cu. ft. After installation, the density was verified by weight. The installation is a messy process, resulting in some scrap insulation. This scrap insulation was collected and weighed. Because it is also a very dusty process, an additional 1% of total insulation used was estimated as the amount of scrap insulation that could not be collected. The scrap weight combined with the

estimated 1% was subtracted from the total amount used, yielding an installed weight of 25.72 lbs. and a density of 3.37 lbs./cu. ft. Thus, for subsequent tests voids were created by removing the same volume of insulation as the fiberglass test volume then verified by weight. Table 7 shows the measurements used to create the accurately sized gaps**.**

Table 7. Amount of cellulose insulation removed

Percent of insulation removed	Weight (lbs)	Area (sq in)	Volume (cu in)
2%	.514	74.4	260.5
5%	1.286	188.6	660.0
.33% (for each distributed gap)	.085	12.6	44.0

Figure 22. Measuring weight of cellulose removed for 2% gap

Figure 23. Measuring weight of cellulose removed for one of the 6 distributed 0.33% gaps

Figures 22 and 23 show the measurement of cellulose removed for the 2% gap and one of the six distributed 0.33% gaps. It should be noted that the scale was adjusted to

display the weight of the cellulose, without the tare weight of the plastic bag. It should also be noted that the scale has a precision of .002 lbs, which is why it is rounded up to .086.

Although this study originally planned to also include open cell polyurethane spray foam insulation, it was excluded because it would not be possible to reinstall insulation in the voids and match the original density. Also, the locations and configurations of the gaps are less likely in typical spray foam insulation applications.

Test Procedure

The procedure between the wall sample tests differed from the procedure between the calibration tests because only a portion of the assembly was changed for each test. After the initial installation of the wall assembly and the attachment of the sensors, the cooling equipment was turned on, and the cold chamber was left undisturbed through out each series of wall sample tests. Between the fiberglass and cellulose series, the cold chamber was opened to ensure that the sensors were still in place and the cooling equipment was operating properly (i.e., the coils were not iced over).

In the hot chamber, the procedure between tests involved turning off the heater, and removing the drywall with the sensors still attched to it. The appropriate amount of insulation was removed or replaced, and the drywall was reattached and resealed to the surround. Due to damage to the drywall, it was replaced with a new sheet, and the sensors were attached to it before the fiberglass sample with 2% horizontal void was tested.

Chapter 4: Findings and Discussion

Calibration Test Series Results

The temperatures and heater power readings from each of the nine tests were plotted against time as shown in Figure 24, which is from the ¾″ C test. For each group of sensors (i.e., hot grid, hot sample, metering wall interior, metering wall exterior, cold grid, and cold sample) an average of all the sensors in that group is plotted at a sampling rate of 0.57 Hz. The green line plots the power consumed by the heater. The power consumption is only shown for the analyzed portion of the test. As this shows, there is a ramp-up period of a few hours before both the hot and cold chambers reach steady temperatures and the power to the heater is in steady intervals. There is a fluctuation range for each of the sensor groups, with the exception of the sensors on the exterior of the metering wall. These peaks and valleys likely represent the cycling of the heating and cooling equipment. This will be examined further in the temperature distribution analysis. Plots for the other calibration tests can be found in Appendix A.

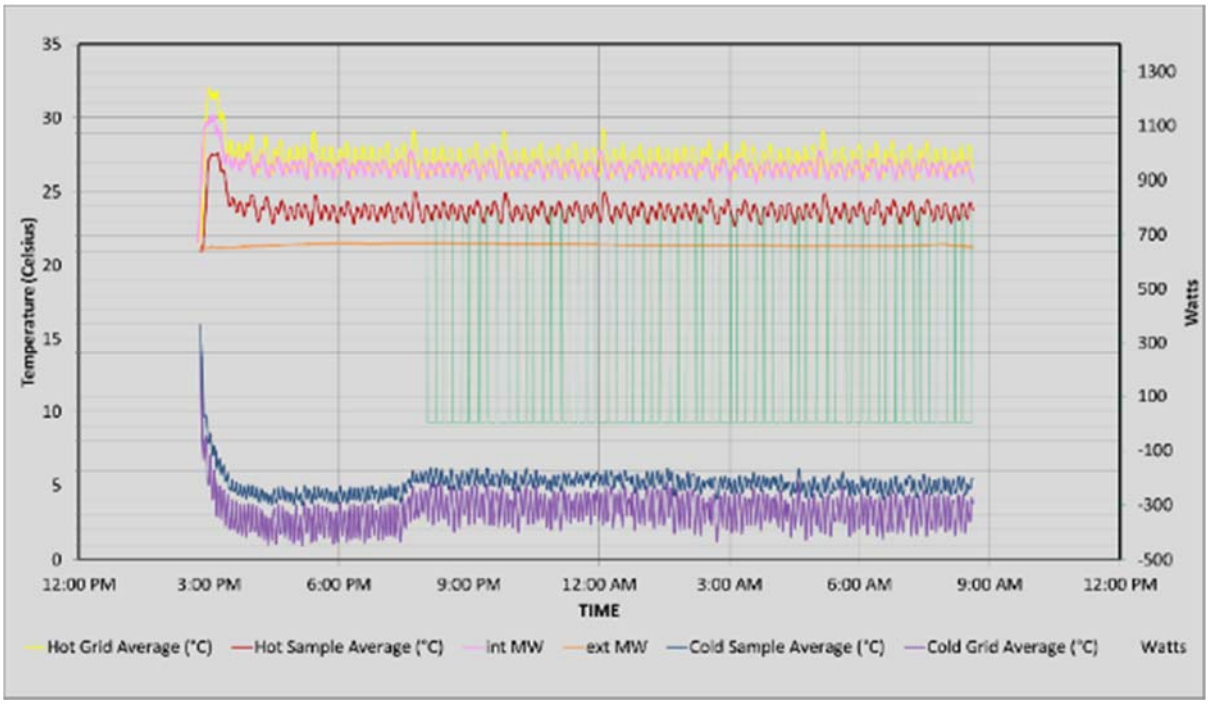

Figure 24. Plotted temperature and wattage over time

Average hot- and cold- side temperatures and heater power are calculated over the equilibrium period. Equations 1, 2, and 3 were used to calculate the overall RSI of the sample. The precision and accuracy of the results were examined. Deviations from the mean are shown in Table 8. Although standard statistics (e.g., standard deviation) can't be applied to this sample because it is an aggregation of three separate distributions, the average deviation has a magnitude of less than 4%, which gives some indication of the reproducibility of R-value determined by the hot box.

Table 8. Calculation of percent deviation from mean

Tested RSI ($m^2 \cdot K/W$)	Mean	dev	% dev
0.7601	0.7542	-0.0059	-0.8%
0.7389		0.0153	2.0%
0.7636		-0.0094	-1.2%
0.8819	0.8136	-0.0683	-8.4%
0.7963		0.0173	2.1%
0.7625		0.0510	6.3%
1.0040	0.9868	-0.0172	-1.7%
0.9210		0.0658	6.7%
1.0354		-0.0486	-4.9%

The calibration test results were then compared to the listed R-value from the manufacturer, as shown in Table 9. There is a substantial discrepancy between the listed and tested RSIs, however, the mean error varies based on the R-value. If this pattern continues, the hot box testing procedure will be more accurate when testing samples with R-values of typical residential wall assemblies. The mean error of the calibration tests was plotted in Figure 25. An exponential fit was applied to the data points, and forecasted the percent error of higher R-value samples. The exponential fit was chosen to provide physically reasonable behavior with errors decreasing with increasing R-value, which could be explained by increased sensitivity to extraneous heat loss not through the sample. A conversion factor was determined by using the equation, $y = -1.56076*e^{(-3.164856x)}$, where x is the RSI and y is the percent error.

Table 9. Calibration test results compared to listed R-value.

Calibration tests	Listed RSI ($m^2 \cdot K/W$)	Tested RSI ($m^2 \cdot K/W$)	% Error	Mean Error
1/2" A	0.5283	0.7601	-30%	-30%
1/2" B	0.5283	0.7389	-28%	
1/2" C	0.5283	0.7636	-31%	
3/4" A	0.6692	0.8819	-24%	-17%
3/4" B	0.6692	0.7963	-16%	
3/4" C	0.6692	0.7625	-12%	
1" A	0.8806	1.0040	-12%	-11%
1" B	0.8806	0.9210	-4%	
1" C	0.8806	1.0354	-15%	

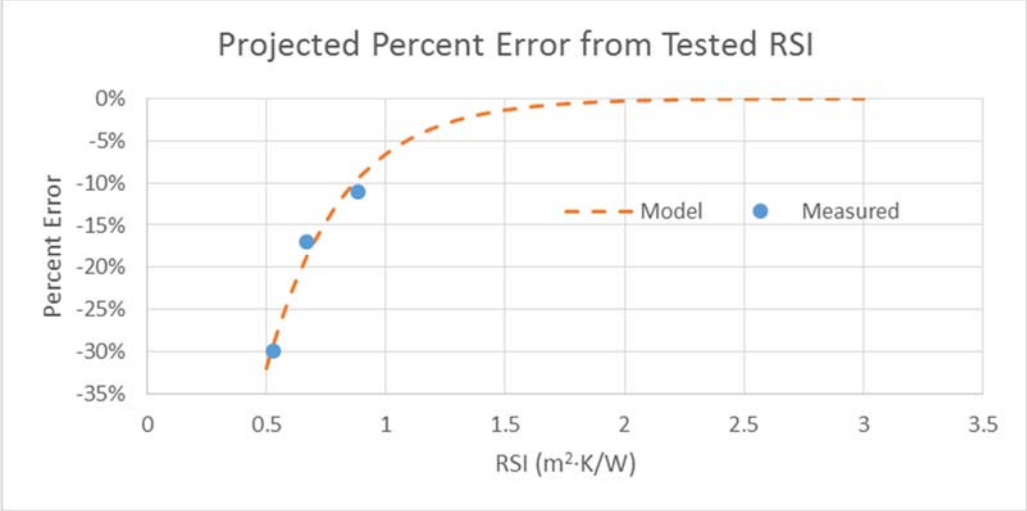

Figure 25. Percent error of tested RSI

In addition, a 2′ x 2′ pieces of the ½″ A, ¾″ A and 1″ B XPS samples were also tested using a Holometrix heat flow meter. The heat flow meter (HFM) is a commercially available apparatus that measures thermal resistance of small scale samples between two heat flux sensors. Although using this type of apparatus is an ASTM approved method of measuring R-value, the results of this particular model may be inaccurate due to the age of the machine

and the possible deterioration of the materials used to calibrate the HFM. A comparison of the listed RSI and RSIs from the HFM and hot box tests are shown in Figure 26.

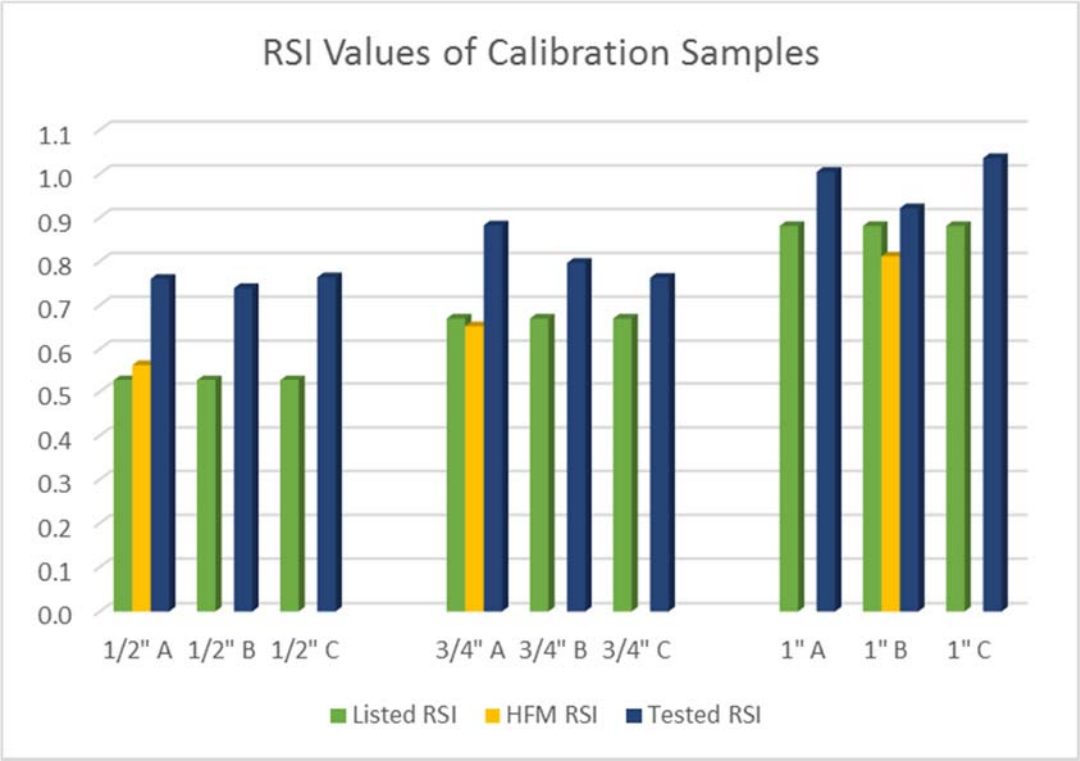

Figure 26. Comparison of RSI ($m^2 \cdot K/W$) from hot box test, heat flow meter, and manufacturer's specifications

Estimated R-Value of Tested Wall Samples

Parallel path calculations were used to estimate the R-value of each tested wall sample. Because this method does not account for the location or distribution of gaps, a comparison of the tested and estimated R-values would indicate the effect of the location and distribution of the gaps on the total thermal resistance of the wall.

The parallel path method for calculating R-value is demonstrated in Table 10. There are 3 parallel paths of heat transfer through a wall assembly: framing, insulation, and gaps.

For each of these paths, the R-value of all other materials remains constant. The only variables that change are the cavity insulation, due to the slight difference in R-value per inch of fiberglass and cellulose, and the percentage of gaps (both highlighted in Table 10). The framing factor is the percent of wood used in a wall assembly. This is used to determine the weighting factor of the R-value for each path of heat transfer. Typically, the framing factor of 2x4 walls with 16 o.c. stud spacing is approximately 25%. However, the actual framing factor of the built wall sample was measured as 17%. This is lower than normal because the wall sample did not include corners, double top plates, ladder framing, or other configurations that require extra lumber. Thus, the estimated R-value of the wall sample with fiberglass insulation and 5% gaps is 13.15 ($ft^2 \cdot °F \cdot hr/Btu$), or RSI - 2.32 ($m^2 \cdot K/W$). Iterative calculations were performed for the two types of insulation and 3 levels of gap percentage, and the resulting R-values are shown in Table 11.

Table 10. Estimated wall assembly R-value calculation with three parallel paths showing variable cells highlighted

	R-value ($ft^2 \cdot °F \cdot hr/Btu$)		
Layer	Framing	Insulation	Gaps
Exterior air film	0.17	0.17	0.17
WRB	0	0	0
OSB	0.62	0.62	0.62
Air space in gap			1
Cavity insulation		15	
Cavity framing	4.38		
drywall	0.45	0.45	0.45
Interior air film	0.68	0.68	0.68
Total R-value	6.295	16.92	2.92
% of Wall	17.00%	78.00%	5.00%
% / R	0.0270	0.0461	0.0171
Sum %/R (U-factor of wall)			0.09023
R-value (1/U) ($ft^2 \cdot °F \cdot hr/Btu$)			**11.08**
		RSI ($m^2 \cdot K/W$)	**1.95**

Table 11. Estimated R-value for wall assemblies based on material and percentage of missing insulation

Wall assembly	Estimated R-value ($m^2 \cdot K/W$)
Fiberglass no gaps	2.32
Fiberglass 2% gaps	2.15
Fiberglass 5% gaps	1.95
Cellulose no gaps	2.13
Cellulose 2% gaps	1.99
Cellulose 5% gaps	1.82

Wall Sample Test Results

An example of the plotted temperature and heater power consumption through a test of the fiberglass wall sample is shown in Figure 27. The same test, 2% horizontal void, in the cellulose series is shown in Figure 28. The temperature and heater power plots from the remaining tests can be found in Appendices B and C. The change in profile of the hot side sensor readings is not likely to be due to the insulation material. Based on the periodicity of the readings, it is more likely that some change happened to the heater.

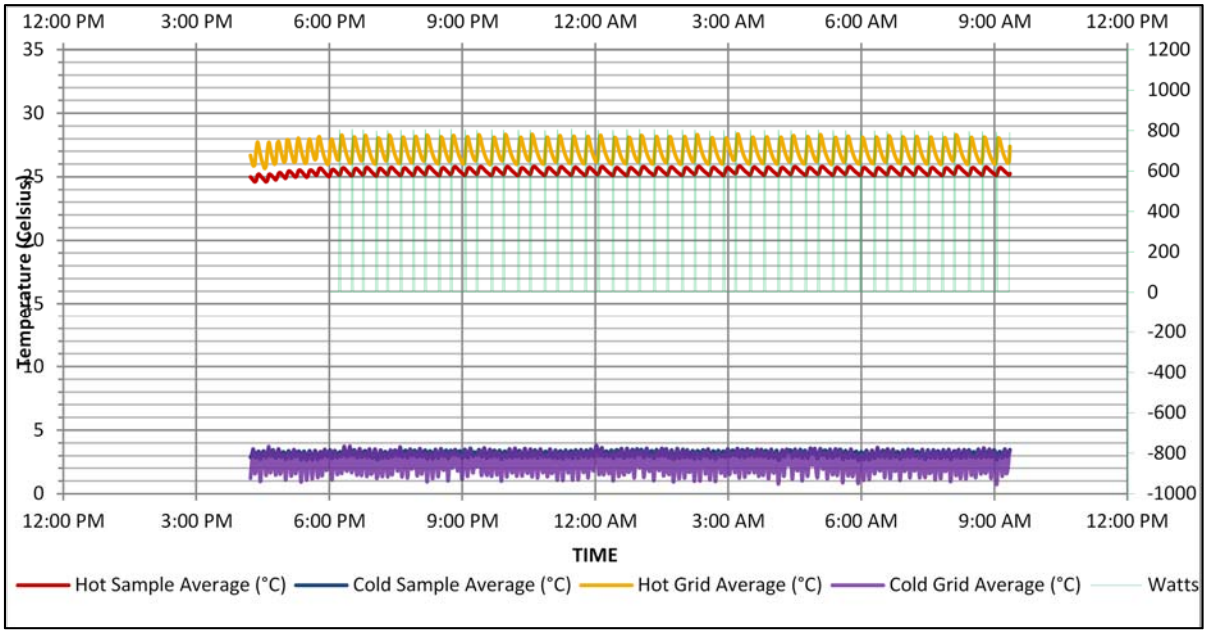

Figure 27. Fiberglass, 2% horizontal gaps

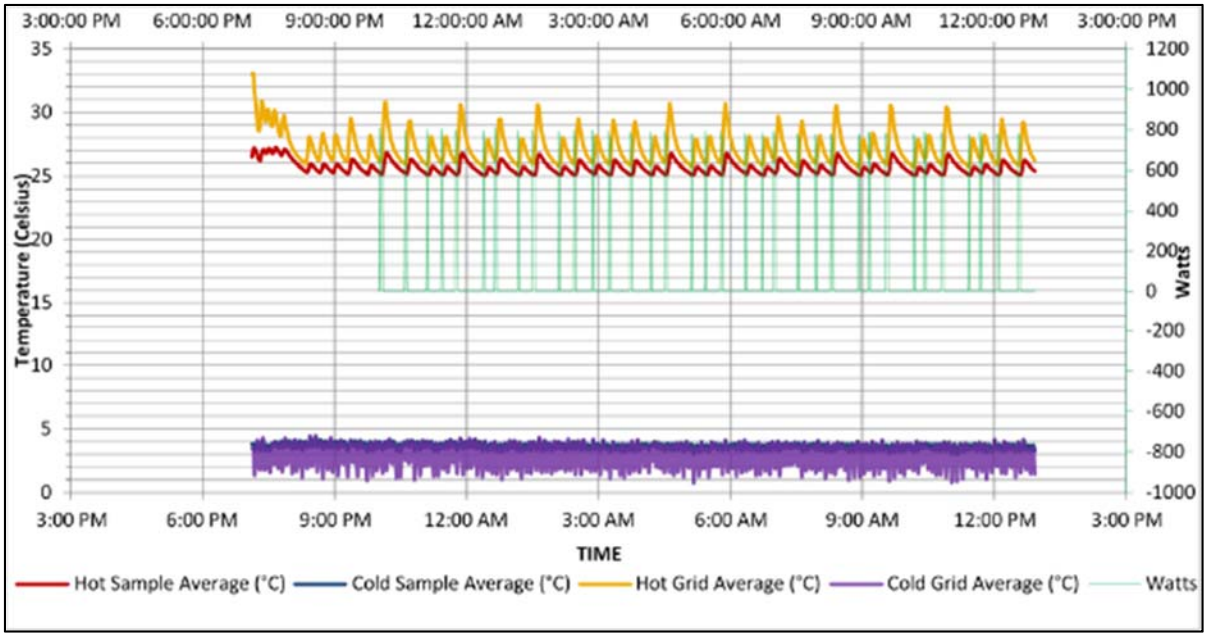

Figure 28. Cellulose 2% horizontal gaps

The empirically determined hot box calibration factor developed from the calibration test results, y=-1.56076*e$^{(-3.164856x)}$, was applied to the R-value from the wall sample tests. The results are shown in Tables 12 and 13. These corrected RSI values were then compared to the estimated RSIs from the parallel path calculations in Table 14.

Table 12. Calibration factors and resulting RSI values for fiberglass tests

Fiberglass	Tested RSI ($m^2 \cdot K/W$)	Calibration factor	Corrected RSI ($m^2 \cdot K/W$)
no gaps	1.442	0.016	1.465
2% horizontal	1.720	0.007	1.731
5% horizontal	1.628	0.009	1.643
no gaps again	1.512	0.013	1.532
2% vertical	1.560	0.011	1.577
2% distributed	1.554	0.011	1.571

Table 13. Calibration factors and resulting RSI values for cellulose tests

Cellulose	Tested RSI ($m^2 \cdot K/W$)	Calibration factor	Corrected RSI ($m^2 \cdot K/W$)
no gaps	1.898	0.004	1.906
2% horizontal	1.599	0.010	1.614
5% horizontal	1.493	0.014	1.514
no gaps again	1.487	0.014	1.508
2% vertical	1.520	0.013	1.539
2% distributed	1.506	0.013	1.526

Table 14. Comparison of measured and estimated RSI values

Wall Assembly	Fiberglass RSI ($m^2 \cdot K/W$)		Cellulose RSI ($m^2 \cdot K/W$)	
	Measured	Estimated	Measured	Estimated
no gaps	1.465	2.32	1.906	2.13
2% horizontal	1.731	2.15	1.614	1.99
5% horizontal	1.643	1.95	1.514	1.82
no gaps again	1.532	2.32	1.508	2.13
2% vertical	1.577	2.15	1.539	1.99
2% distributed	1.571	2.15	1.526	1.99

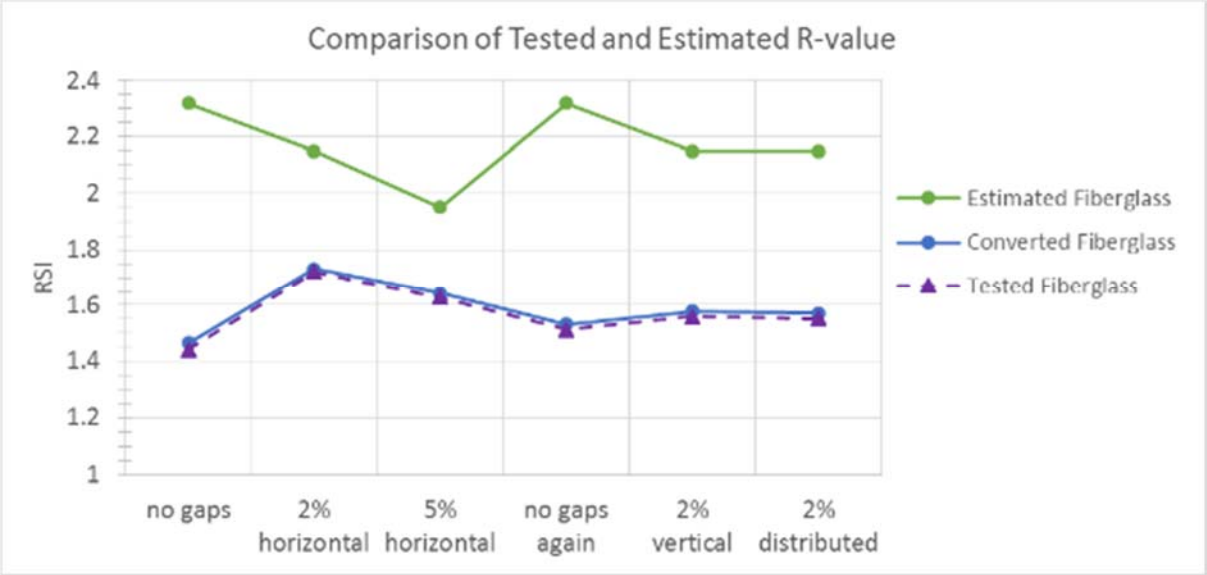

Figure 29. Comparison of estimated, tested, and converted RSIs of fiberglass wall samples

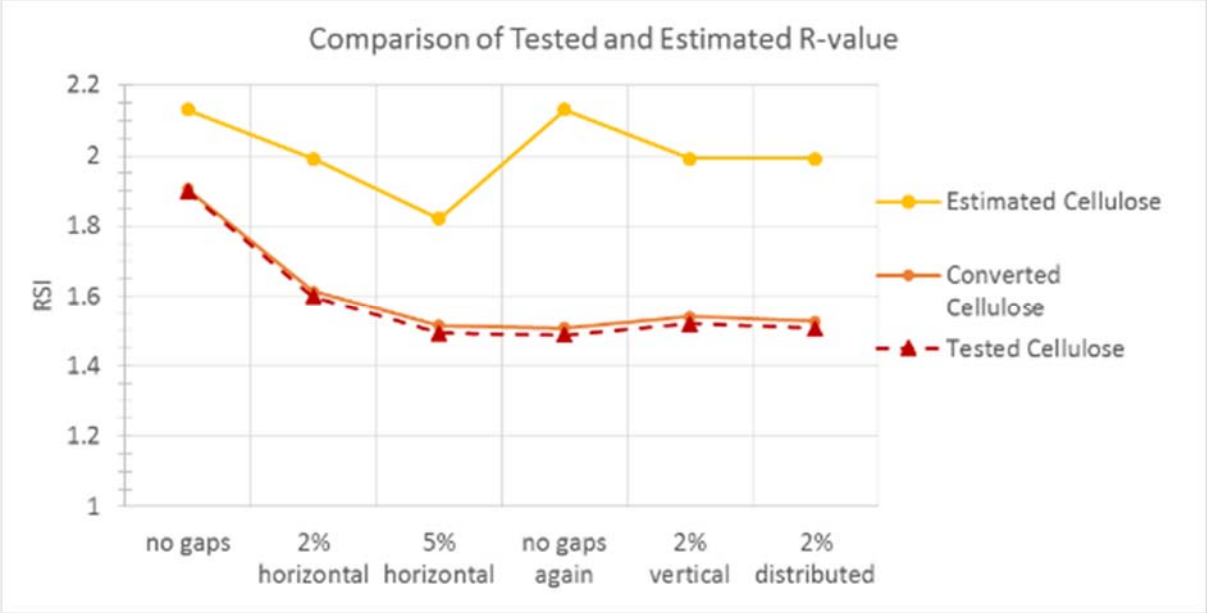

Figure 30. Comparison of estimated, tested, and converted RSIs of cellulose wall samples

Although the correction factors yield RSI values comparable to the estimated RSIs in some cases, there are clearly problems with these test results, namely with the tests when no insulation was removed. For each type of insulation, these tests should have the highest RSIs

and be equivalent. Ultimately, the fiberglass and cellulose tests and subsequent calculations were inconclusive. The resulting R-values varied from the estimated R-values in a manner that indicates unreliable data.

The unexpected results from the test series of wall samples could be due to a number of factors. Although the gaps in the insulation were controlled, there may have been a gap between the stud / insulation layer and the drywall. This would have been caused by the drywall not being fully attached to the studs. The proper installation procedures were followed, using drywall screws every 16″. However, due to the tight dimensions of the sample surround, it was not possible to ensure full contact between the drywall and studs. This may have been more of an issue with the fiberglass series. The cellulose series of tests produced the more realistic results.

Extraneous Heat Transfer

As discussed in Chapter 3, there are three alternative paths of heat transfer other than through the sample being tested. The heat transfer from the hot chamber to ambient space (Q_{mw}) and the heat transfer through the wall dividing the hot and cold chambers (Q_{dw}) were analyzed to further characterize the hot box. As expected, Q_{mw} varied depending on the ambient temperature outside the hot box. As the temperature differential across the metering box exterior wall increased, the amount of heat transferred, as a percentage of total energy (Q), also increased. This is shown in Figure 31.

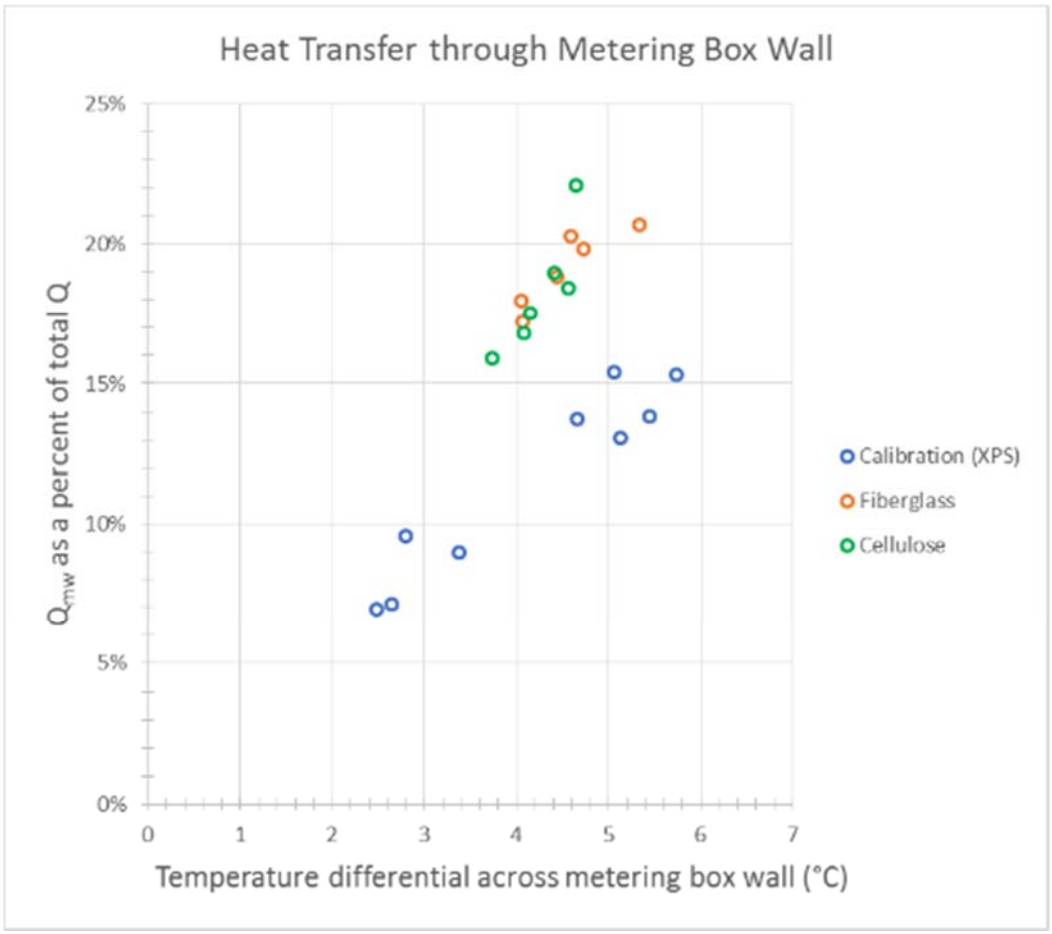

Figure 31. Percentage of total heat transfer in comparison to ΔT across metering box wall

Similarly, Q_{dw} as a percentage of Q increased as the RSI of the sample increased. In other words, as the resistance to heat flow of the sample becomes closer to that of the dividing wall, the total heat transfer from the hot chamber is less concentrated through the sample. This is shown in Figure 32.

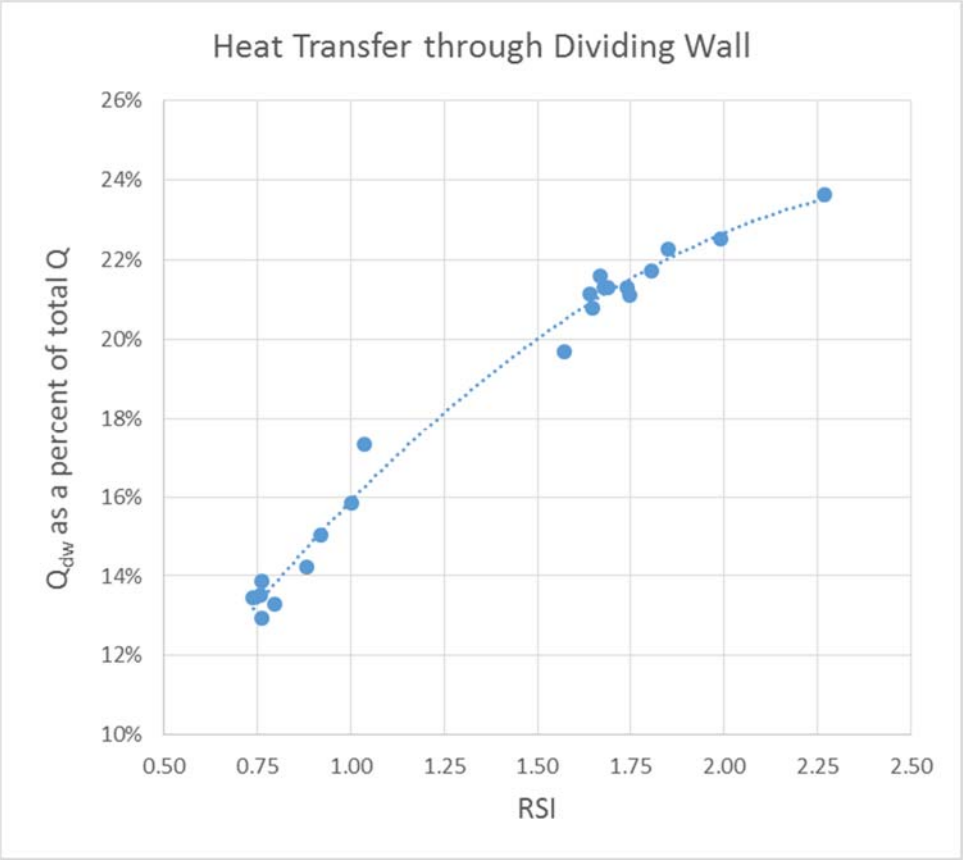

Figure 32. Percentage of heat transfer through dividing wall in comparison to RSI of sample

Temperature Distribution

The temperature distribution across the sample and the three-dimensional grid was analyzed for each of the sample wall tests, as well as some of the calibration tests. There are at least two factors affecting this distribution. The first is the location of the heating and cooling equipment. Although baffles were installed to mitigate radiant heat transfer, the temperature could not be equalized throughout the hot or cold chambers. This can be seen in Figure 33. The visual representation of this distribution in three dimensions may not be immediately clear. The top group of cells represent the 20 sensors attached directly to the sample. The second group of 12 cells represents the row of hanging sensors closest to the

sample. The third group represents the row of sensors further from the sample (Refer to Figure 3). The cells are color coded based on average temperature over the equilibrium phase of the test. Red represents the highest temperature among the sensors represented in each figure, and yellow represents the lowest temperature. In Figure 33, the warmest area of the sample is at the bottom, which is where the heater is located. Throughout the three-dimensional grid there is also some stratification.

		23.34	23.04	23.39	23.30	23.29		
		23.87	23.32	23.14	24.60	23.79		
		23.36	23.88	23.69	24.58	23.77		
		24.44	24.68	25.70	24.63	24.66		
28.53		28.33		26.99		28.13		
27.41		27.06		28.13		27.35		
26.49		26.85		26.67		26.63		
28.48		28.07		27.13		28.13		
27.55		27.12		28.16		27.40		
26.50		26.56		26.60		26.69		

Figure 33. Hot chamber temperature distribution for 1/2 inch XPS

An analysis of the sample wall tests shows that the temperature distribution is also affected by the size location of the insulation gaps. Figures 34 through 38 show the results of the fiberglass wall series. It is especially clear in the case of the 5% horizontal gap, that the lowest temperature corresponds with the location of the gap. Without further testing and/or different methods of heating and cooling the chambers, it is not clear which of these factors (location of heater or location of gap) has the most impact on the temperature distribution, or whether there are other factors involved. The results of the cellulose tests show similar distributions, and can be found in Appendix D.

		25.48	25.47	25.01	25.47	25.13	
		25.74	25.71	25.11	25.77	25.46	
		25.85	25.96	25.35	25.82	25.75	
		25.91	25.97	25.59	25.92	25.39	
27.78		27.73		26.97		27.58	
27.15		26.97		27.58		27.13	
26.47		26.78		26.68		26.61	
27.80		27.54		26.98		27.59	
27.29		27.07		27.61		27.20	
26.52		26.71		26.75		26.75	

Figure 34. Fiberglass no gaps temperature distribution

		25.32	25.49	24.92	25.36	25.02	
		25.59	25.63	24.60	25.67	25.34	
		25.71	25.84	25.26	25.70	25.62	
		25.75	25.83	25.46	25.74	25.22	
27.65		27.52		26.83		27.40	
27.00		26.80		27.39		27.00	
26.39		26.65		26.58		26.49	
27.64		27.39		26.83		27.42	
27.14		26.91		27.43		27.04	
26.41		26.54		26.59		26.63	

Figure 35. Fiberglass 2% horizontal gap temperature distribution

		25.34	25.45	24.83	25.37	25.03	
		25.59	25.62	23.93	25.67	25.34	
		25.74	25.84	25.35	25.67	25.61	
		25.70	25.89	25.58	25.75	25.24	
27.53		27.41		26.78		27.32	
26.95		26.77		27.30		26.94	
26.38		26.57		26.55		26.48	
27.52		27.28		26.79		27.33	
27.06		26.84		27.34		27.00	
26.40		26.48		26.56		26.59	

Figure 36. Fiberglass 5% horizontal gap temperature distribution

		25.33	25.19	23.91	25.24	24.99	
		25.55	25.58	24.72	25.54	25.32	
		25.59	25.69	24.91	25.78	25.59	
		25.55	25.74	25.53	25.67	25.32	
27.59		27.38		26.79		27.30	
26.91		26.89		27.27		26.97	
26.36		26.86		26.59		26.50	
27.53		27.29		26.80		27.32	
27.06		26.89		27.35		26.97	
26.40		26.45		26.60		26.61	

Figure 37. Fiberglass 2% vertical gap temperature distribution

		23.34	23.03	23.36	23.26	23.28	
		23.88	23.31	23.12	24.58	23.77	
		23.36	23.88	23.68	24.57	23.77	
		24.44	24.69	25.59	24.63	24.67	
28.56		28.37		27.01		28.17	
27.43		27.08		28.16		27.37	
26.51		26.86		26.68		26.65	
28.51		28.11		27.16		28.16	
27.58		27.15		28.19		27.43	
26.51		26.58		26.61		26.71	

Figure 38. Fiberglass 2% distributed gaps temperature distribution

Figure 39 shows the temperature distribution over the hot sample sensors during a calibration test. Plotting each sensor separately shows that the position of the sensor has a significant effect on its temperature relative to the other hot sample sensors. For example, hot sample sensor #5 (HS5) records the highest temperature at every timestamp. Of all the sample sensors, HS5 is the closest to the heater. The wattage of the heater is represented by the bold grey line. It is apparent that while the temperatures of all of the sensors rise when the heater turns on, they also tend to stay in the same relative order.

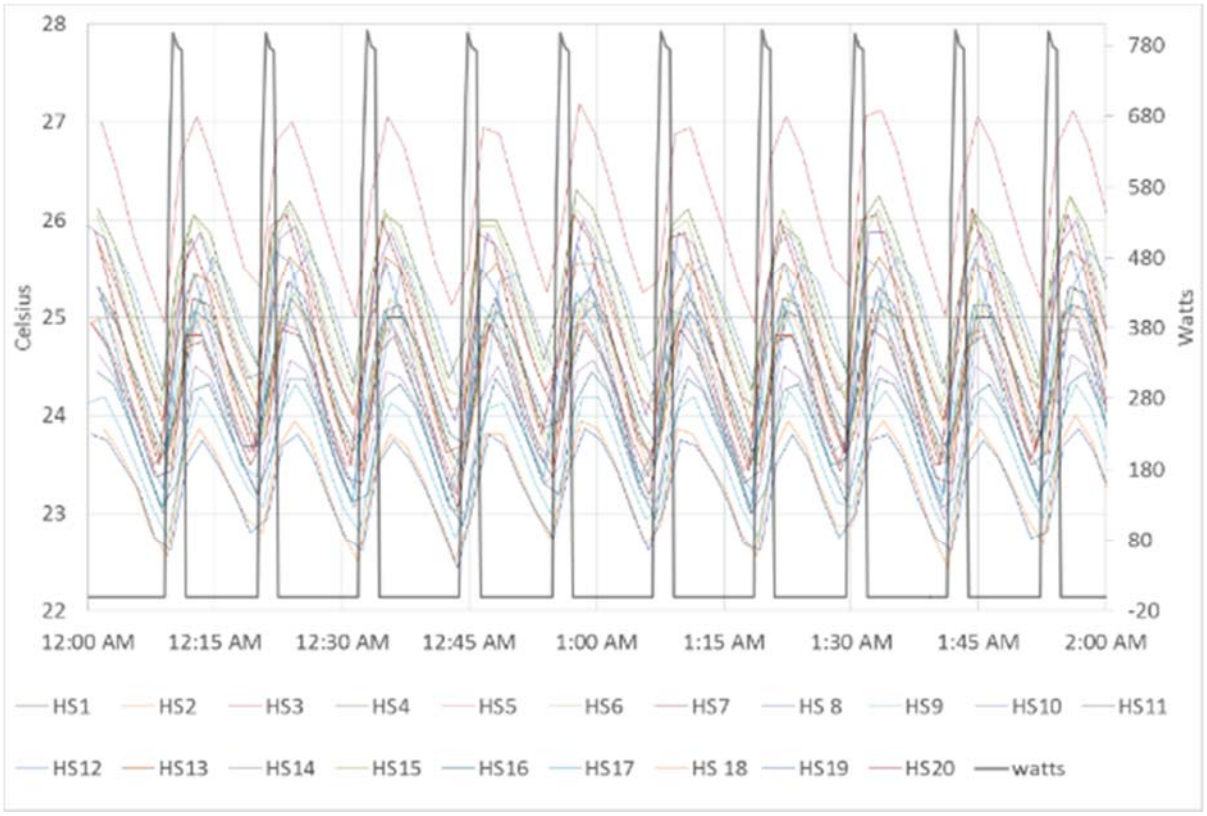

Figure 39. Temperature of individual hot sample sensors

Chapter 5: Conclusions

This study sought to develop a better understanding of how the size and position of insulation voids affect the overall R-value of a wall assembly. In the process, an apparatus was developed to perform empirical tests in order to answer this question. The results of the calibration process and the sample wall tests yielded an understanding of the characterization of the hot box and its applicability to testing various building assemblies. The results of the calibration tests showed encouraging precision, although the results did not match the listed R-values.

Research Questions

1. In standard residential construction, how do voids in different types of wall insulation affect the total thermal resistance of the wall assembly?
2. What is the correlation between the size of the void, as a percentage of the total insulated area, and the magnitude of the reduction in thermal resistance? Is there a difference in this correlation between two widely used residential insulation materials?
3. How does the distribution of voids affect total R-value? For example, does a 2% void concentrated in one place affect the total R-value differently than smaller voids that add up to 2% distributed across the sample? Or, do voids of the same size, but different locations and orientations affect the total R-value differently?

These research questions cannot be conclusively answered because the resulting R-values from the wall sample tests indicated unreliable data The variation between the first R-value of the first ‘no gaps’ test and the second ‘no gaps’ test clearly showed a lack of precision that was not evident in the calibration tests. This suggests that there is a flaw in the testing procedure that affects wall assemblies, but not single materials. While the results of

the wall samples were inconclusive, the calibration process and analysis provides direction for what further work would be required for the hot box to produce accurate results for wall assemblies with a range of R-values.

The data from the wall sample tests do provide useful information about the ability of the hot box to measure localized temperature differentials and the distribution of temperature across a sample and through the three-dimensional grid. The tests with concentrated gaps clearly showed evidence of the location of the gaps through a comparison of the temperature readings of each sensor.

Future Work

Future work to be done involves improving the hot box to minimize the possibility that test specimens are installed incorrectly. Essentially, the test procedure needs to control for unintended factor variation so that the results can be confidently attributed to the intended factor variation. As discussed in Chapter Four, one of these unintended changes was likely a gap between the drywall and the stud / insulation assembly. Another factor that inadvertently changed for each test was the amount of caulk used to seal the final layer of the hot side of the wall assembly (i.e., the drywall). The framing, OSB sheathing, and WRB were each sealed and left undisturbed throughout the testing procedure. The drywall, however, was removed between each test and resealed. The method of resealing was consistent, but changes in the amount of caulk used or how fully it had cured before the test began could have had an unknown effect on the total R-value of the assembly.

One approach to avoid this potential irregularity would be to employ a reusable gasket that could be attached along the border of both the hot and cold sides of the assembly. Another improvement would be to replace the 2″ XPS that create the surround with an

insulation material of similar R-value, but with a skin making it less susceptible to damage. It is very difficult, if not impossible, to repeatedly remove and reattach the drywall without causing some damage to the unprotected insulation of the surround.

These tests and subsequent analyses also made it clear that both the cycling of the heating and cooling equipment and the position of the equipment have unintended effect on the tests. Future work could include developing alternative heating and cooling methods that produce a more even chamber temperature.

The most useful work to be done in light of the results of this study is to continue the calibration tests with samples of higher R-values. This would provide the opportunity to confirm the calculated correction factor which forecasted the percent error for higher R-value samples. If this can be confirmed, the hot box can be confidently used to measure total thermal resistance of wall assemblies within the calibrated range of R-values.

References

al-Homoud, M. S. (2005). Performance characteristics and practical applications of common building thermal insulation materials. *Building and Environment, 40,* 353-366. doi:10.1016/j.buildenc.2004.05.013

Asdrubali, F., & Baldinelli, G. (2011). Thermal transmittance measurements with the hot box method: Calibration, experimental procedures, and uncertainty analyses of three different approaches. *Energy and Buildings, 43,* 1618-1626. doi:10.1016/j.enbuild.2011.03.005

ASTM International. (2005). *Standard test method for thermal performance of building materials and envelope assemblies by means of hot box apparatus* (Designation C 1363 – 05). West Conshohocken, PA: ASTM International.

ASTM International (2010). *Standard practice for selecting temperatures for evaluating and reporting thermal properties of thermal insulation* (Designation C1058/ C1058M – 10). West Conshohocken, PA: ASTM International.

Baum, K. (2010). *Evaluating the uniformity of distribution of dense-pack cellulose insulation as a retrofit in enclosed wall cavities*, Unpublished PowerPoint, Department of Technology and Environmental Design, Appalachian State University, Boone, North Carolina.

Brown, W. C., Bomberg, M. T., Ullett, J. M., & Rasmussen, J. (1993) Measured thermal resistance of frame walls with defects in the installation of mineral fibre insulation. *Journal of Building Physics, 16,* 318-339. doi: 10.1177/1097639301600404

Bynum, R. T. (2001). *Insulation handbook.* New York, NY: McGraw Hill.

Cammerer, J., Spitzner, M., Treiber, G., Schmitt, H., & Heinz, S. (2003). Settling and acceptable size of gaps in loose-fill thermal insulation in walls. In J. Carmeliet, H. Hens, & G. Vermier (Eds.), *Research in building physics: proceedings of the 2nd international conference on building physics* (pp.545-553). Leuven, Belgium: Taylor & Francis.

CertainTeed Corporation. (2014), *Sustainable insulation specification sheet: fiber glass building insulation.* Code No. 30-45-001. Valley Forge, PA: CertainTeed Corporation.

Christian, J. E., & Kosny, J. (1997). Wall R-values that tell it like it is. *Home Energy, March/April 1997,* 15-20.

Christian, J. E., Kosny, J., Desjarlais, A. O., & Childs, P. W. (1998). The whole wall thermal performance calculator–on the net. In *Proceedings*, *Thermal Performance of the Exterior Envelopes of Buildings VII*, 287-299. Atlanta, GA: American Society of Heating, Refrigerating and Air-Conditioning Engineers.

Dow Building Solutions. (n.d.). *Manufacturer's Insulation Fact Sheet: Extruded Polystyrene Foam Home Insulation Products*. Form No. 179-07335-1008MCK. Retrieved from: http://msdssearch.dow.com/PublishedLiteratureDOWCOM/dh_040b/0901b8038040bb48.pdf?filepath=styrofoam/pdfs/noreg/179-07335.pdf&fromPage=GetDoc.

Green Building Advisor. (2012). *Grading the installation quality of insulation.* Retrieved from http://www.greenbuildingadvisor.com/blogs/dept/building-science/grading-installation-quality-insulation

Green Building Advisor. (2013). *Spray foam insulation: Open and closed cell.* Retrieved from http://www.greenbuildingadvisor.com/green-basics/spray-foam-insulation-open-and-closed-cell

GreenFiber. (2015). *Dry dense-packing wall and floor assemblies.* WI-6.19-16 Rev G. Charlotte, NC: US GreenFiber LLC.

Harley, B. (2005). Insulation inspections for home energy ratings. *Home Energy, January/February 2005*: 20-23.

Harley, B. (2007). *Insulation quality and compliance assessments: Field inspections for insulation*. Retrieved from http://web.ornl.gov/sci/buildings/2012/2007%20B10%20papers/127_Harley.pdf

Harvey, L. D. D. (2006). *A handbook on low-energy buildings and district-energy systems: Fundamentals, techniques and examples*. London: Earthscan.

International Code Council & American Society of Heating, Refrigerating and Air-Conditioning Engineers. (2011). *2012 International Energy Conservation Code: And, ANSI/ASHRAE/IES standard 90.1-2010, energy standard for buildings except low-rise residential buildings.* Washington, D.C: International Code Council.

Jelle, B. (2011). Traditional, state-of-the-art and future thermal building insulation materials and solutions—properties, requirements and possibilities. *Energy and Buildings, 43*: 2549–2563. doi: 10.1016/j.enbuild.2011.05.015

Kanarek, D., & Dobsevage, M. (Producers). (2015). *Dense-packed cellulose* [online video]. Retrieved from http://www.greenbuildingadvisor.com/green-basics/video-dense-packed-cellulose-1

Karamanos, A., Papadopoulos, A. M., & Anastaselo, D. (2004*). Heat transfer phenomena in fibrous insulating materials*. In *Proceedings, WSEAS/IASME International Conference on Heat and Mass Transfer*. 1–12. Corfu, Greece: World Scientific and Engineering Academy and Society.

Lavine, A. G., Rucker J. L., & Wilkes, K. E., (1983). Flanking loss calibration for a calibrated hot box. In F. Govan, D. Greason, and J. McAllister (Eds.), *Thermal insulation, materials, and systems for energy conservation in the '80s* (pp. 234-247). Baltimore, MD: American Society for Testing and Measurement.

Lawton, M., Roppel, P., Fookes, D., St. Hilaire, A. T., & Schoonhoven, D. (n.d.). *Real R-value of exterior insulated wall assemblies.* Retrieved from: http://c.ymcdn.com/sites/www.nibs.org/resource/resmgr/BEST/BEST1_029.pdf

Oak Ridge National Laboratory. (2004). *Rotatable guarded hot box*. Retrieved from http://web.ornl.gov/sci/roofs+walls/AWT/Ref/WMDIntro.htm

Residential Energy Services Network. (2014). *What is RESNET?* Retrieved from http://www.resnet.us/about/what-is-resnet

Straube, J. (2009). RR-0901: *Thermal metrics for high performance enclosure walls: The limitations of R-value*. Retrieved from http://www.buildingscience.com/documents/reports/rr-0901-thermal-metrics-high-performance-walls-limitations-r-value/view

Thorsell, T., & Bomberg, M. (2008). Integrated methodology for evaluation of energy performance of building enclosures: Part II - examples of application to residential walls. *Journal of Building Physics, 32*, 49-65. doi:10.1177/1744259108093317

Trethowen, H.A. (1991), Sensitivity of insulated wall and ceiling cavities to workmanship. *Journal of Building Physics, 15,* 172-179. doi:10.1177/109719639101500205

United States Department of Energy. (2012a). *Buildings energy data book*. Retrieved from http://buildingsdatabook.eren.doe.gov/ChapterIntro1.aspx

United States Department of Energy. (2012b). *Types of insulation*. Retrieved from http://energy.gov/energysaver/articles/types-insulation

Appendix A:

Calibration Tests

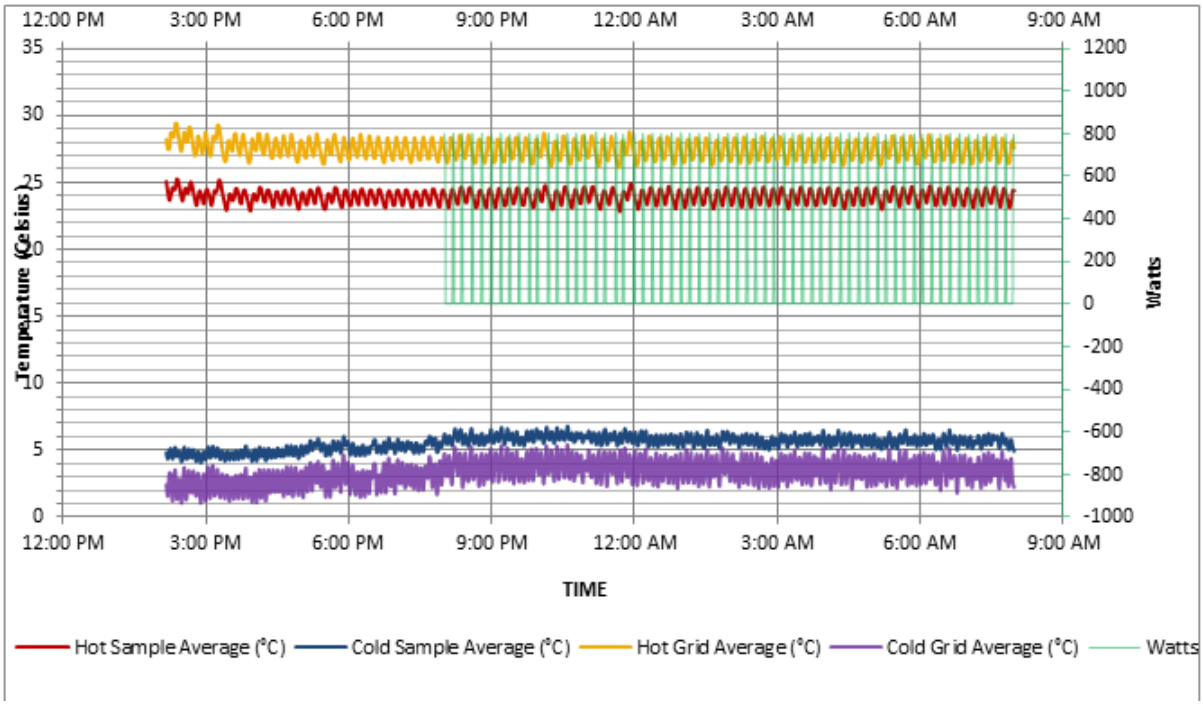

Figure A1. ½″ XPS A

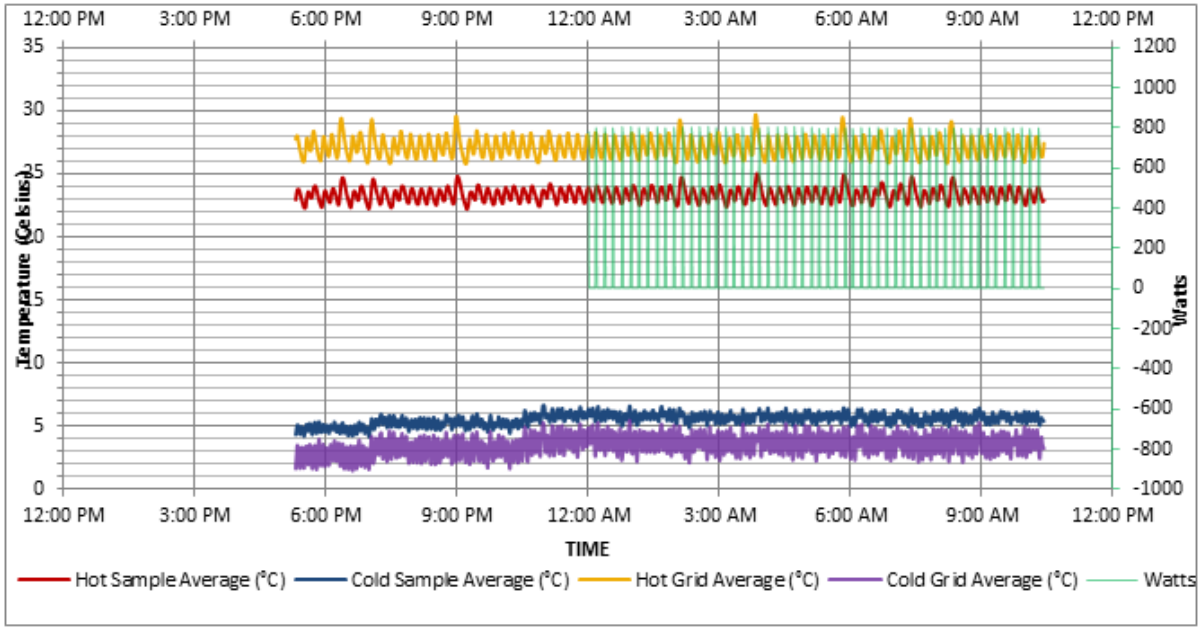

Figure A2. ½″ XPS B

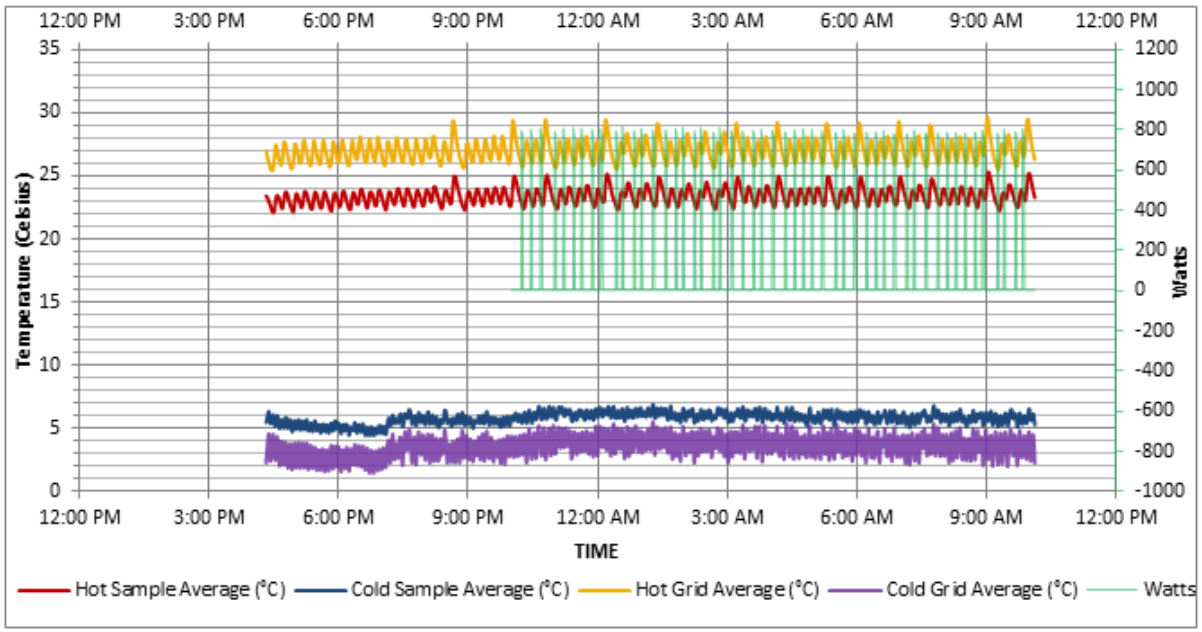

Figure A3. ½″ XPS C

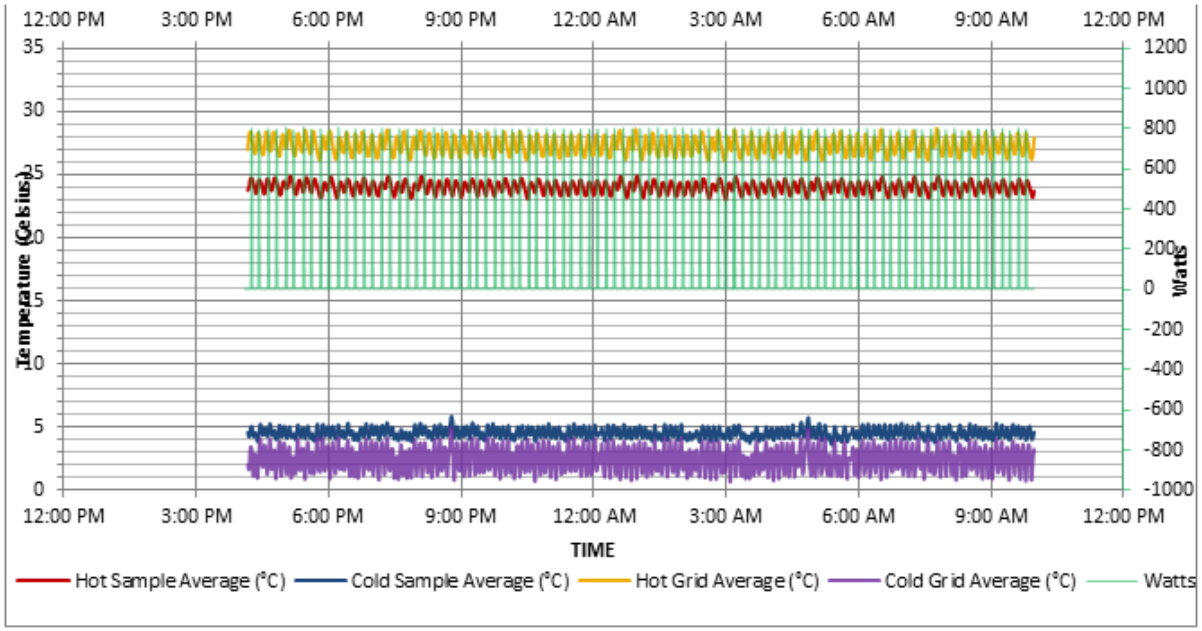

Figure A4. ¾″ XPS A

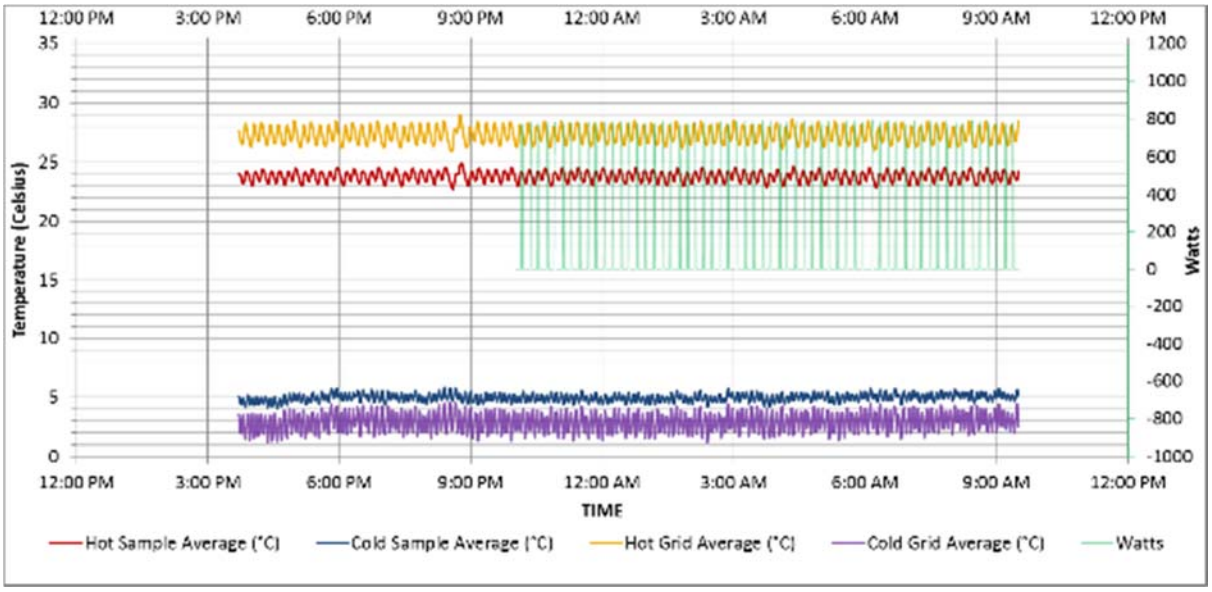

Figure A5. ¾″ XPS B

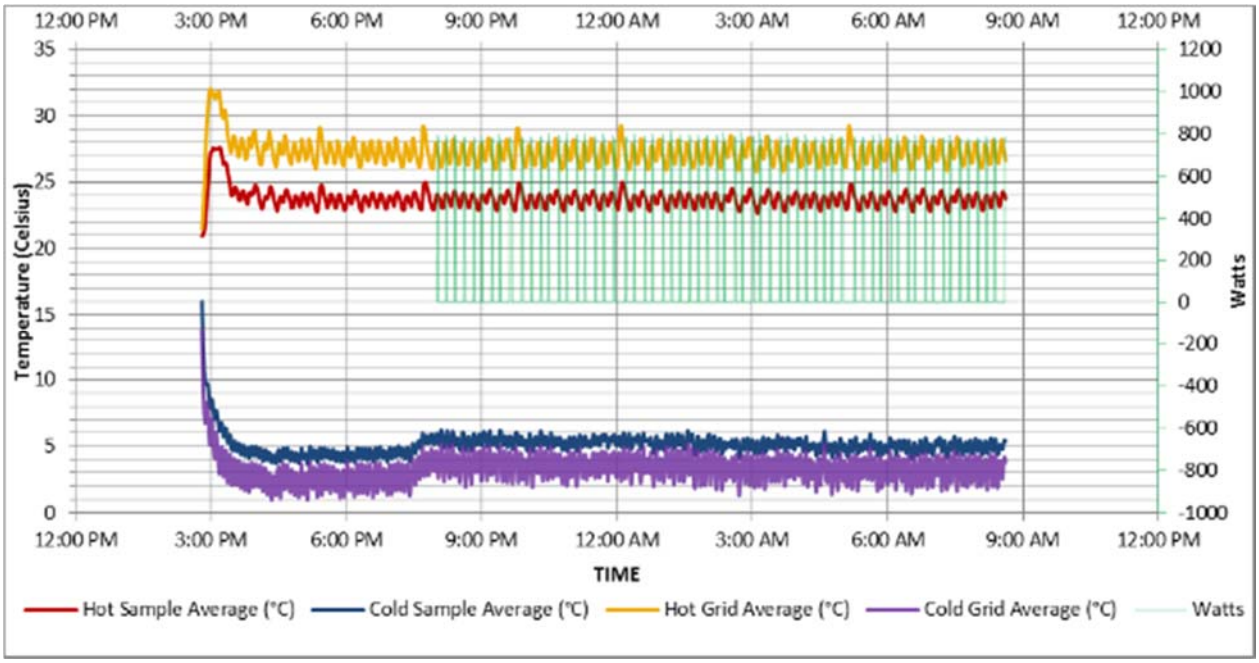

Figure A6. ¾″ XPS C

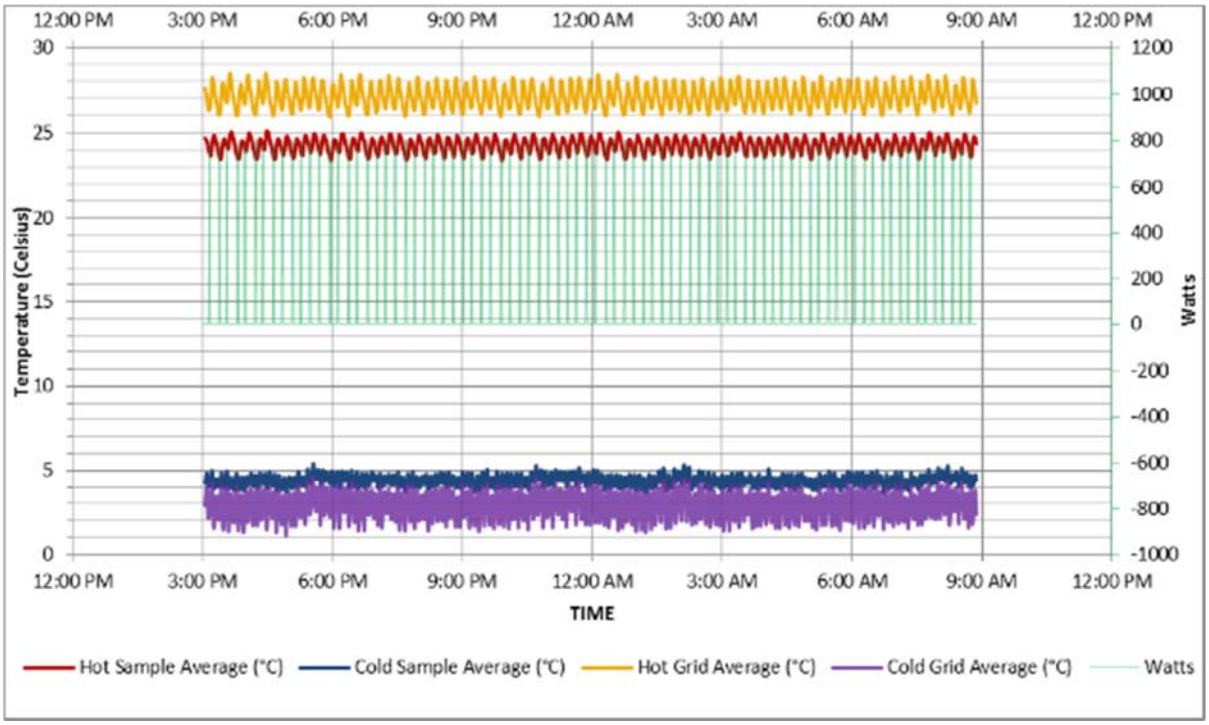

Figure A7. 1″ XPS A

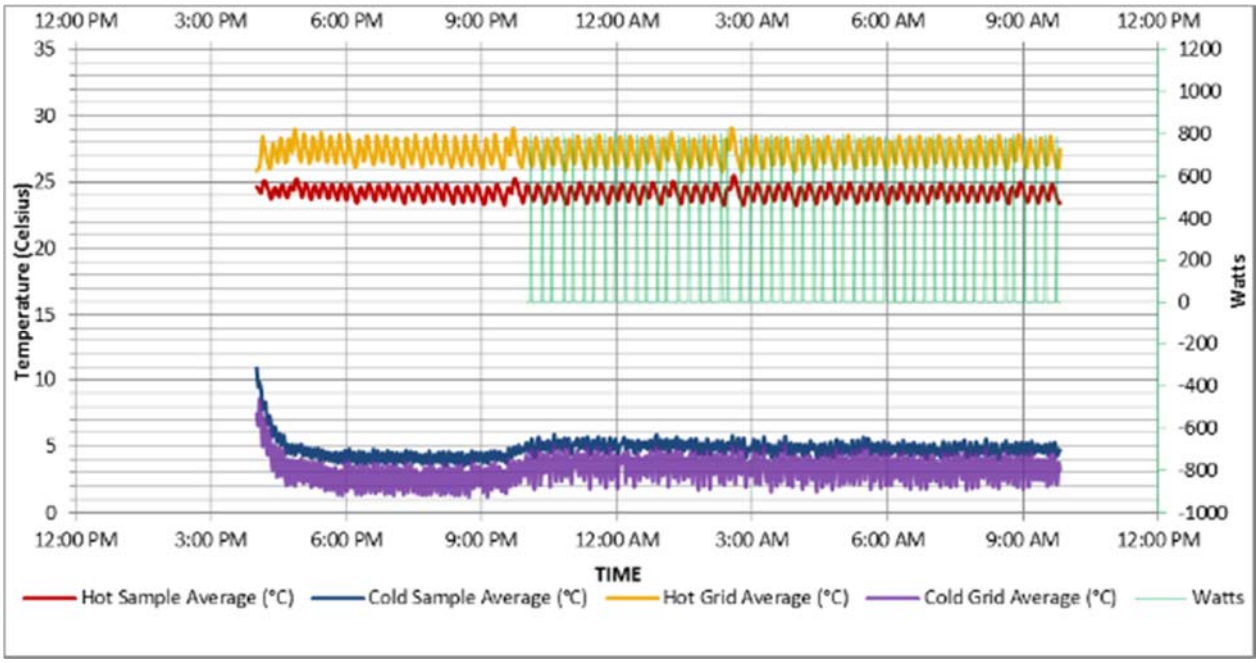

Figure A8. 1″ XPS B

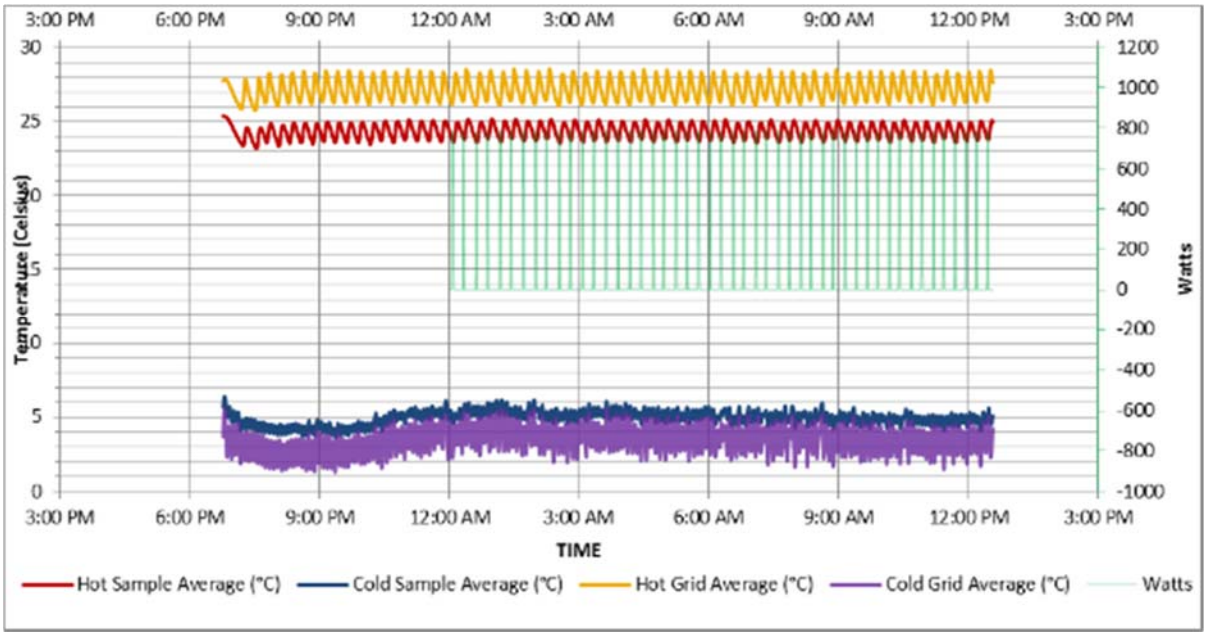

Figure A9. 1″ XPS C

Appendix B:

Fiberglass Tests

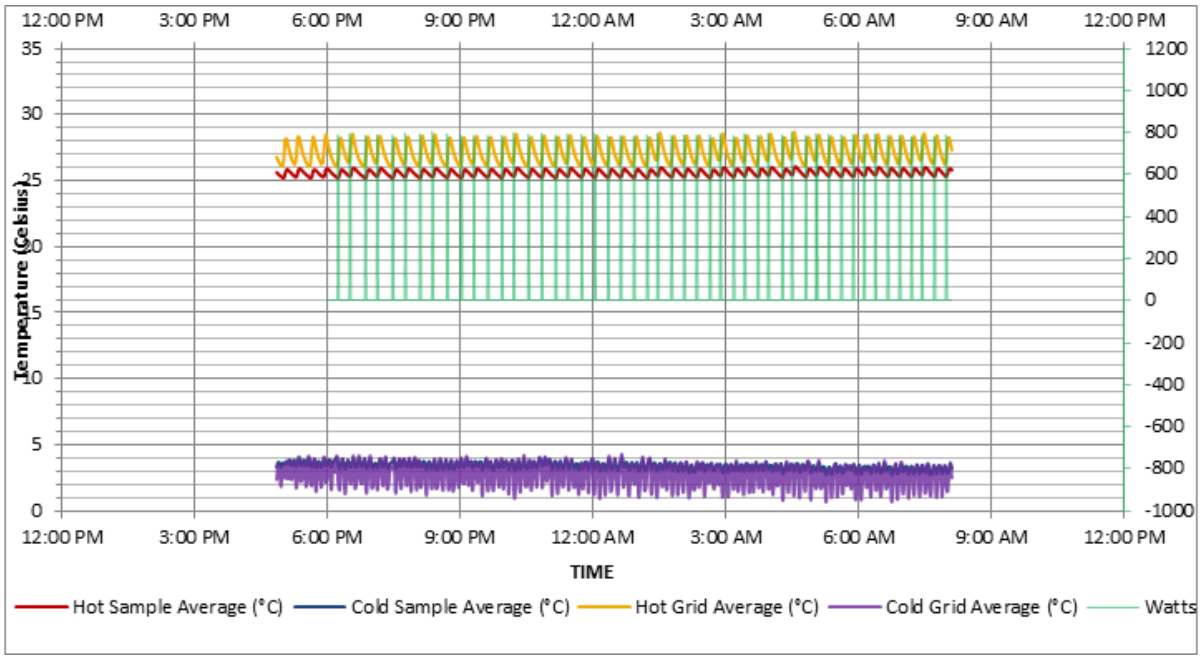

Figure B1. Fiberglass no gaps

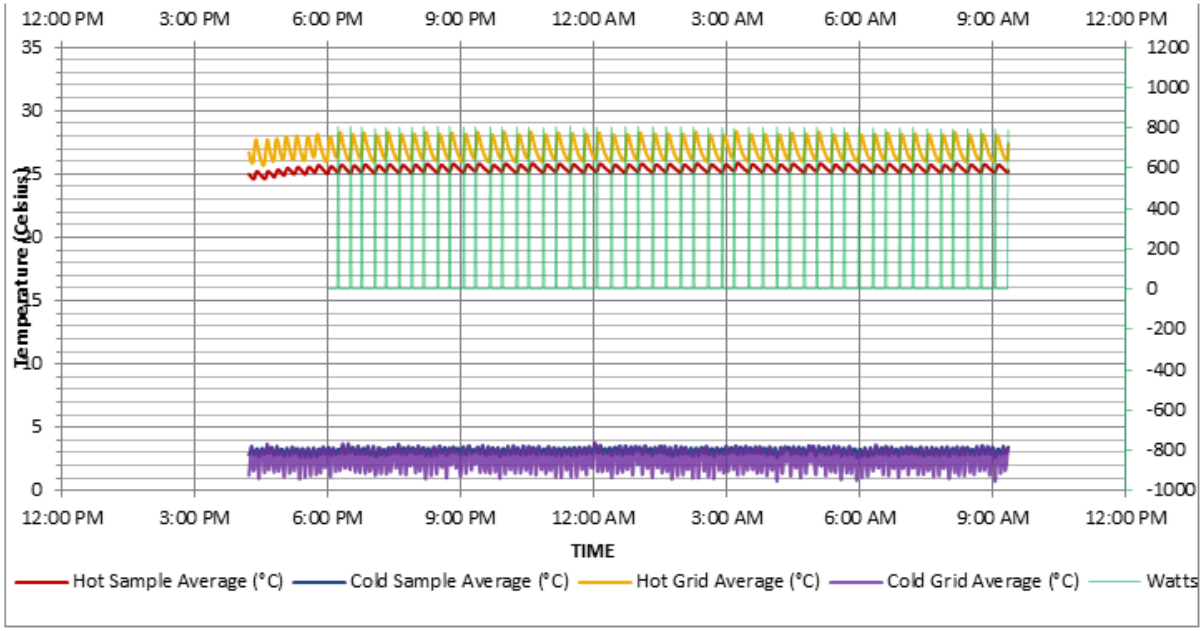

Figure B2. Fiberglass 2% horizontal gap

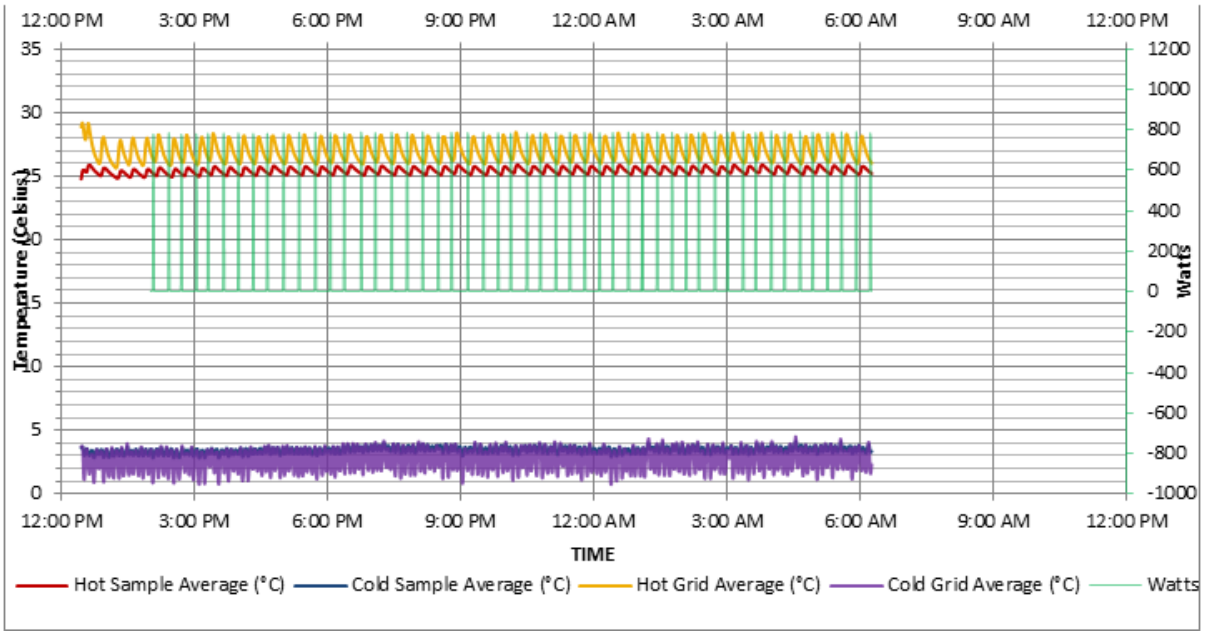

Figure B3. Fiberglass 5% horizontal gap

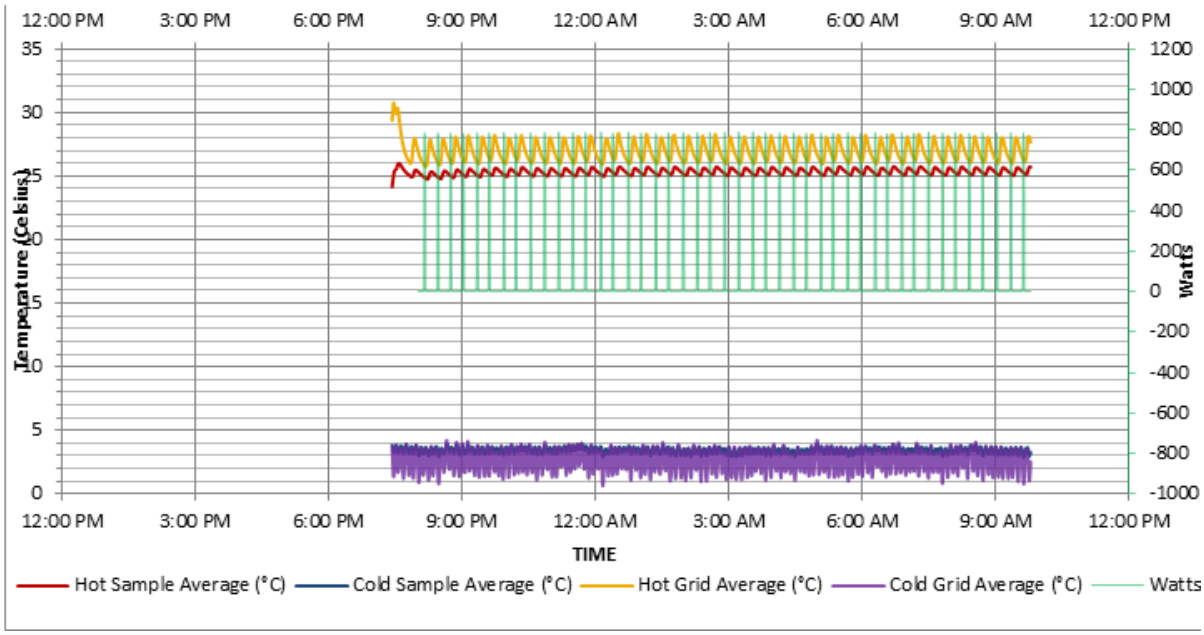

Figure B4. Fiberglass 2% horizontal gap

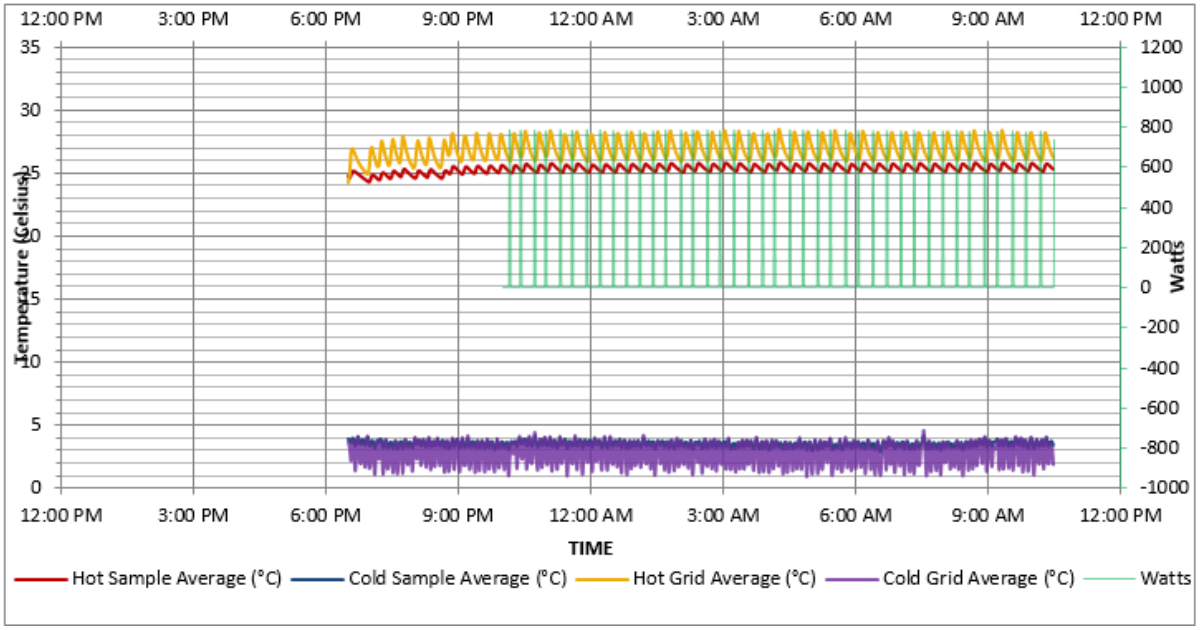

Figure B5. Fiberglass 2% distributed gaps

Appendix C:

Cellulose Tests

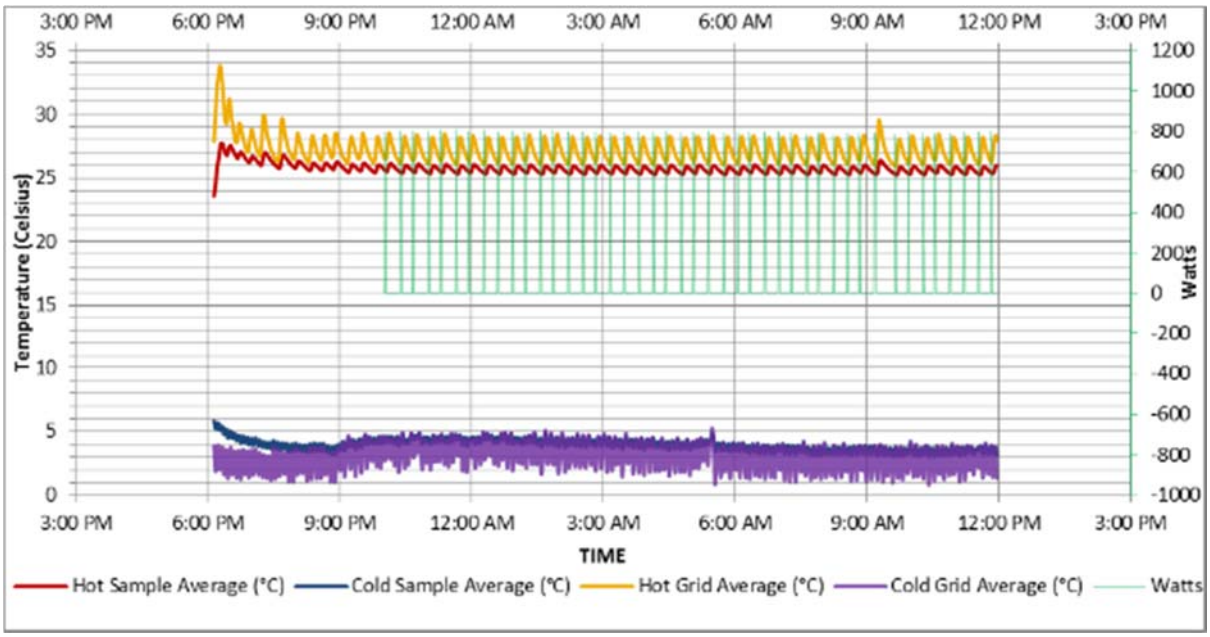

Figure C1. Cellulose no gaps

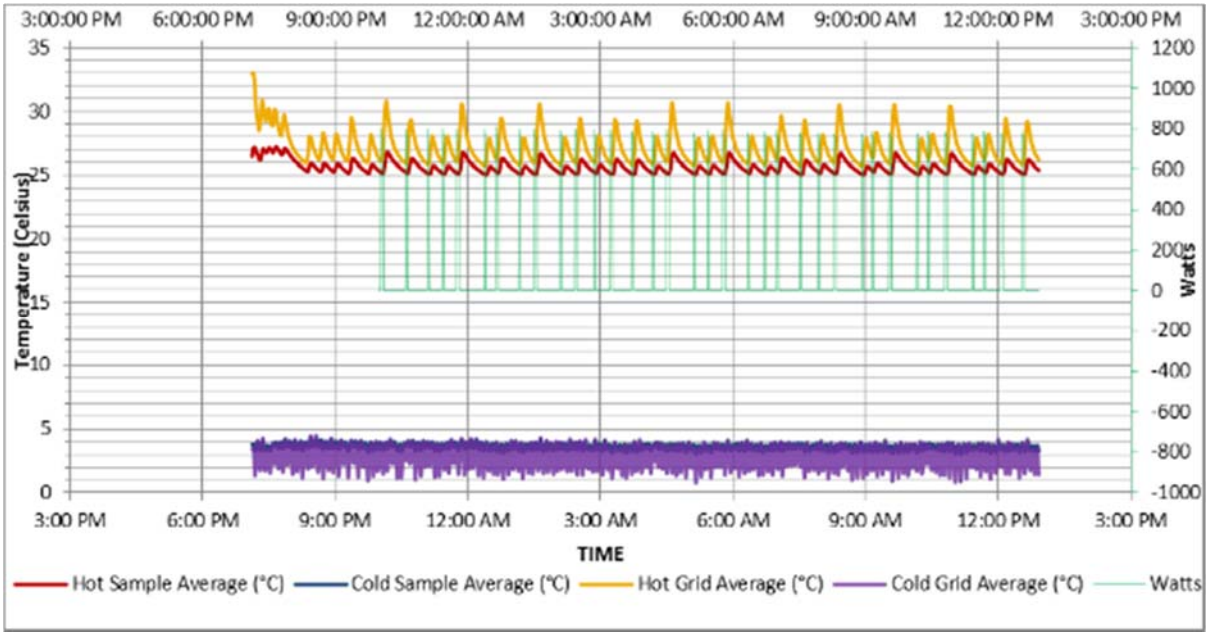

Figure C2. Cellulose 2% horizontal gap

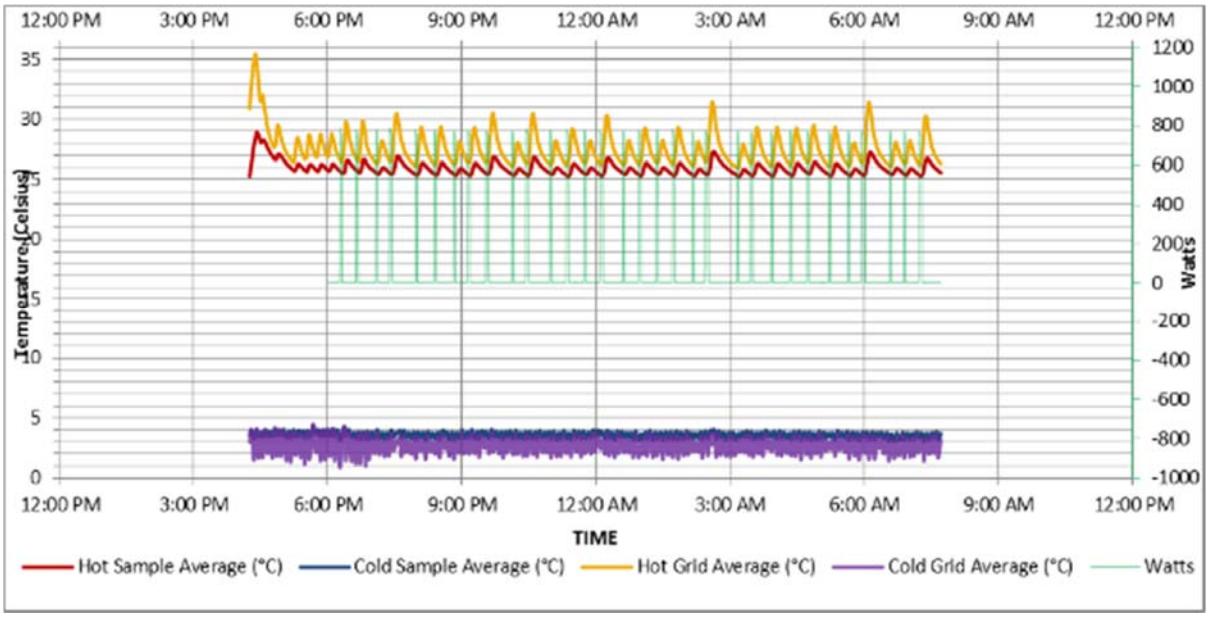

Figure C3. Cellulose 5% horizontal gap

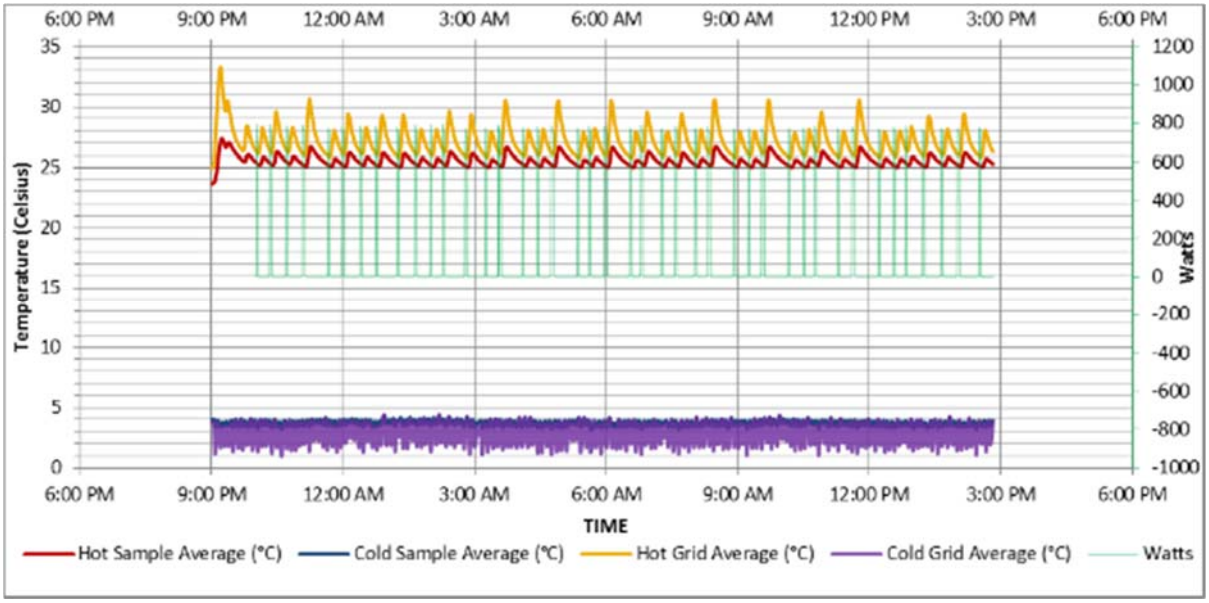

Figure C4. Cellulose 2% vertical gap

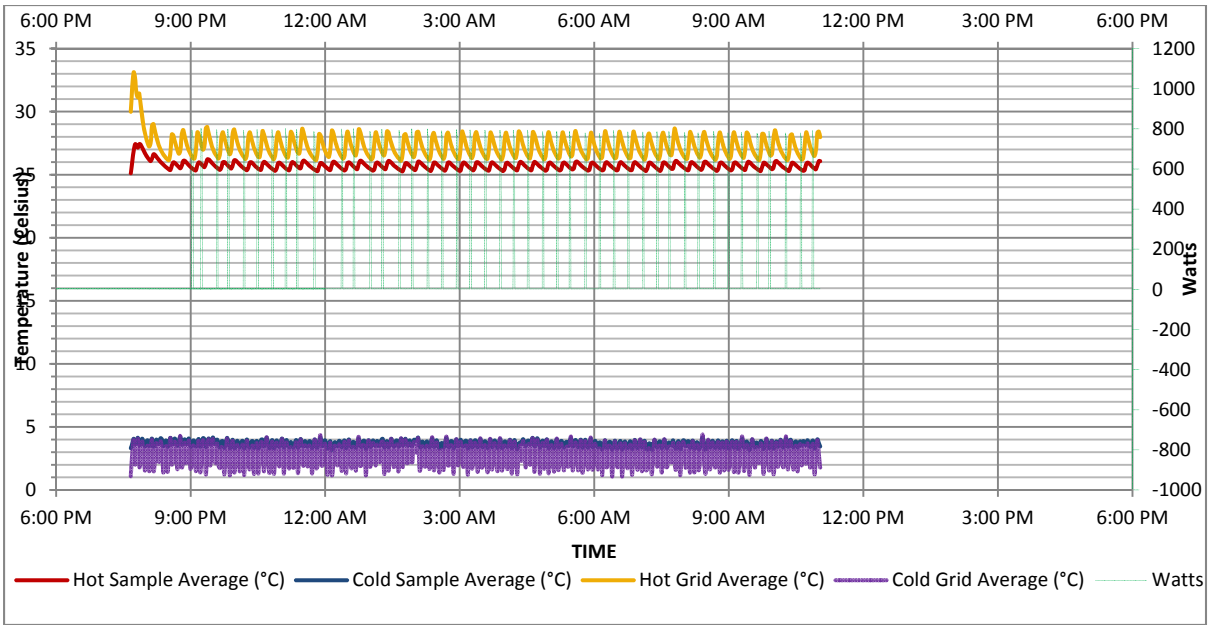

Figure C5. Cellulose 2% distributed gaps

Appendix D:

Temperature Distribution in Cellulose Tests

		25.38	25.45	25.11	25.41	25.25	
		25.73	25.72	25.47	25.70	25.51	
		25.84	25.86	25.64	25.94	25.74	
		25.87	25.97	25.87	25.94	25.68	
27.63		27.52		26.92		27.44	
27.07		26.94		27.42		27.08	
26.49		26.77		26.67		26.58	
27.57		27.35		26.90		27.41	
27.20		27.00		27.46		27.05	
26.51		26.60		26.70		26.72	

Figure 7. Cellulose no gaps temperature distribution

		25.34	25.48	25.07	25.40	25.17	
		25.72	25.71	25.02	25.70	25.51	
		25.82	25.82	25.50	25.94	25.77	
		25.80	25.90	25.77	25.95	25.66	
27.63		27.51		26.90		27.41	
27.03		27.04		27.39		27.09	
26.50		27.10		26.68		26.61	
27.55		27.35		26.90		27.39	
27.20		27.00		27.43		27.03	
26.53		26.61		26.70		26.74	

Figure 8. Cellulose 2% horizontal gap temperature distribution

		25.67	25.74	25.31	25.70	25.47	
		26.03	26.01	24.38	25.98	25.82	
		26.15	26.16	25.85	26.26	26.04	
		26.16	26.27	26.08	26.24	26.00	
28.08		27.97		27.31		27.87	
27.50		27.28		27.86		27.48	
26.81		27.27		26.99		26.95	
28.02		27.76		27.30		27.84	
27.65		27.36		27.89		27.45	
26.85		26.89		27.02		27.09	

Figure 9. Cellulose 5% horizontal gap temperature distribution

		25.43	25.45	24.12	25.39	25.21	
		25.72	25.69	24.89	25.65	25.47	
		25.80	25.83	25.29	25.92	25.72	
		25.78	26.01	25.92	25.98	25.74	
27.69		27.61		26.97		27.52	
27.15		26.96		27.49		27.12	
26.52		26.88		26.68		26.65	
27.63		27.40		26.96		27.47	
27.30		27.06		27.51		27.13	
26.56		26.56		26.71		26.77	

Figure 10. Cellulose 2% vertical gap temperature distribution

		25.56	25.45	25.08	25.28	25.29	
		25.79	25.74	25.39	25.72	25.51	
		25.82	25.89	25.61	25.98	25.81	
		25.89	26.03	25.88	26.01	25.76	
27.80		27.65		27.01		27.58	
27.19		27.06		27.53		27.18	
26.61		27.16		26.79		26.69	
27.71		27.48		27.01		27.54	
27.34		27.13		27.59		27.17	
26.65		26.66		26.80		26.83	

Figure 11. Cellulose 2% distributed gap temperature distribution

Vita

Helen “Lena” Whistler Burkett was born in Fort Worth, Texas, to Vicki Whistler and Jeff Burkett. She graduated from Trinity Valley School in 2002. She attended Hendrix College, where she earned a Bachelor of Arts degree in Philosophy in 2007. After graduating, Ms. Burkett served two years as an AmeriCorps Service Member with construction based non-profit organizations. She became a Senior Home Energy Professional at Clinton Climate Initiative, performing building diagnostics and energy analyses. In 2013, she began her graduate studies in the department of Sustainable Technology and the Built Environment at Appalachian State University. In 2015, she was awarded the Most Outstanding Graduate Student Award in Building Science and she earned a Master of Science degree with a concentration in Building Science.